Published for SISSA by Springer

Received: October 7, 2016
Accepted: December 26, 2016
Published: January 4, 2017

# Simultaneous explanation of the $R_K$ and $R_{D^{(*)}}$ puzzles: a model analysis

**Bhubanjyoti Bhattacharya,**[a,b] **Alakabha Datta,**[c,d] **Jean-Pascal Guévin,**[a] **David London**[a] **and Ryoutaro Watanabe**[a,e]

[a] *Physique des Particules, Université de Montréal, C.P. 6128, succ. centre-ville, Montréal, QC, H3C 3J7 Canada*
[b] *Department of Physics and Astronomy, Wayne State University, Detroit, MI 48201, U.S.A.*
[c] *Department of Physics and Astronomy, University of Mississippi, 108 Lewis Hall, Oxford, MS 38677-1848, U.S.A.*
[d] *Department of Physics and Astronomy, 2505 Correa Rd, University of Hawaii, Honolulu, Hi 96826, U.S.A.*
[e] *Center for Theoretical Physics of the Universe, Institute for Basic Science (IBS), Daejeon 305-811, Republic of Korea*

*E-mail:* bhujyo@wayne.edu, datta@phy.olemiss.edu, jean-pascal.guevin@umontreal.ca, london@lps.umontreal.ca, watanabe@lps.umontreal.ca

Abstract: $R_K$ and $R_{D^{(*)}}$ are two $B$-decay measurements that presently exhibit discrepancies with the SM. Recently, using an effective field theory approach, it was demonstrated that a new-physics model can simultaneously explain both the $R_K$ and $R_{D^{(*)}}$ puzzles. There are two UV completions that can give rise to the effective Lagrangian: (i) $VB$: a vector boson that transforms as an $SU(2)_L$ triplet, as in the SM, (ii) $U_1$: an $SU(2)_L$-singlet vector leptoquark. In this paper, we examine these models individually. A key point is that $VB$ contributes to $B_s^0$-$\bar{B}_s^0$ mixing and $\tau \to 3\mu$, while $U_1$ does not. We show that, when constraints from these processes are taken into account, the $VB$ model is just barely viable. It predicts $\mathcal{B}(\tau^- \to \mu^-\mu^+\mu^-) \simeq 2.1 \times 10^{-8}$. This is measurable at Belle II and LHCb, and therefore constitutes a smoking-gun signal of $VB$. For $U_1$, there are several observables that may point to this model. Perhaps the most interesting is the lepton-flavor-violating decay $\Upsilon(3S) \to \mu\tau$, which has previously been overlooked in the literature. $U_1$ predicts $\mathcal{B}(\Upsilon(3S) \to \mu\tau)|_{\rm max} = 8.0 \times 10^{-7}$. Thus, if a large value of $\mathcal{B}(\Upsilon(3S) \to \mu\tau)$ is observed — and this should be measurable at Belle II — the $U_1$ model would be indicated.

Keywords: Phenomenological Models

ArXiv ePrint: 1609.09078



doi:10.1007/JHEP01(2017)015

## Contents



JHEP01(2017)015

## 1 Introduction

At present, there are several measurements of $B$ decays that may indicate the presence of physics beyond the standard model (SM):

1. $b \to s\mu^+\mu^-$: the LHCb Collaboration has made measurements of $B \to K^*\mu^+\mu^-$ [1, 2] that deviate from the SM predictions [3]. The Belle Collaboration finds similar results [4]. The main discrepancy is in the angular observable $P_5'$ [5]. The significance of the discrepancy depends on the assumptions about the theoretical hadronic uncertainties [6–8]. Indeed, it has been recently argued [9] that, by including non-factorizable power corrections, the experimental results can be reproduced within the SM. However, the latest fits to the data [10, 11], which take into account the hadronic uncertainties, find that a discrepancy is still present. It may reach the $4\sigma$ level.

   The LHCb Collaboration has also measured the branching fraction and performed an angular analysis of $B_s^0 \to \phi\mu^+\mu^-$ [12, 13]. They find a $3.5\sigma$ disagreement with the predictions of the SM, which are based on lattice QCD [14, 15] and QCD sum rules [16].

2. $R_K$: the LHCb Collaboration has found a hint of lepton non-universality. They measured the ratio $R_K \equiv \mathcal{B}(B^+ \to K^+\mu^+\mu^-)/\mathcal{B}(B^+ \to K^+e^+e^-)$ in the dilepton invariant mass-squared range $1\,\text{GeV}^2 \le q^2 \le 6\,\text{GeV}^2$ [17], and found

$$R_K^{\text{expt}} = 0.745^{+0.090}_{-0.074}\ (\text{stat}) \pm 0.036\ (\text{syst})\,. \tag{1.1}$$

   This differs from the SM prediction of $R_K^{\text{SM}} = 1 \pm 0.01$ [18] by $2.6\sigma$, and is referred to as the $R_K$ puzzle.

3. $R_{D^{(*)}}$: the charged-current decays $\bar{B} \to D^{(*)}\ell^-\bar{\nu}_\ell$ have been measured by the BaBar [19], Belle [20] and LHCb [21] Collaborations. It is found that the values of the ratios $R_{D^{(*)}} \equiv \mathcal{B}(\bar{B} \to D^{(*)}\tau^-\bar{\nu}_\tau)/\mathcal{B}(\bar{B} \to D^{(*)}\ell^-\bar{\nu}_\ell)$ $(\ell = e, \mu)$ considerably exceed their SM predictions. Assuming Gaussian distributions, and taking correlations into account, the experimental results and theoretical predictions can be combined to yield [22, 23]

$$R_D^{\text{ratio}} \equiv \frac{R_D^{\text{expt}}}{R_D^{\text{SM}}} = 1.29 \pm 0.17\ , \qquad R_{D^*}^{\text{ratio}} \equiv \frac{R_{D^*}^{\text{expt}}}{R_{D^*}^{\text{SM}}} = 1.28 \pm 0.09\,. \tag{1.2}$$

   The measured values of $R_D$ and $R_{D^*}$ represent deviations from the SM of $1.7\sigma$ and $3.1\sigma$, respectively. These are known as the $R_D$ and $R_{D^*}$ puzzles.

It must be stressed that, while the discrepancies in point 1 have some amount of theoretical input, those in points 2 and 3 are quite clean. As such, the $R_K$ and $R_{D^{(*)}}$ puzzles provide very intriguing hints of new physics (NP).[1]

[1] Note that, while the $R_K$ and $R_{D^{(*)}}$ puzzles require lepton-non-universal NP, this is not necessarily true for point 1, see ref. [24] for example.



JHEP01(2017)015

In ref. [25], Hiller and Schmaltz searched for a NP explanation of the $R_K$ puzzle. They performed a model-independent analysis of $b \to s\ell^+\ell^-$, considering NP operators of the form $(\bar{s}\mathcal{O}b)(\bar{\ell}\mathcal{O}'\ell)$, where $\mathcal{O}$ and $\mathcal{O}'$ span all Lorentz structures. They found that the only NP operator that can reproduce the experimental value of $R_K$ is of $(V-A)\times(V-A)$ form: $(\bar{s}_L\gamma_\mu b_L)(\bar{\ell}_L\gamma^\mu\ell_L)$. Subsequent fits [26–28], which included both the $B \to K^*\mu^+\mu^-$ and $R_K$ data, confirmed that such a NP operator can also account for the $P_5'$ discrepancy. To be specific, $b \to s\mu^+\mu^-$ transitions are defined via the effective Hamiltonian

$$\begin{aligned} H_{\text{eff}} &= -\frac{\alpha G_F}{\sqrt{2}\pi} V_{tb}V_{ts}^* \sum_{a=9,10} \left(C_a O_a + C_a' O_a'\right) , \\ O_{9(10)} &= [\bar{s}_L\gamma_\mu b_L][\bar{\mu}\gamma^\mu(\gamma_5)\mu] , \end{aligned} \tag{1.3}$$

where the primed operators are obtained by replacing $L$ with $R$. The Wilson coefficients $C_a^{(\prime)}$ include both SM and NP contributions. In the fits it was shown that a NP contribution to $b \to s\mu^+\mu^-$ is required; one of the possible solutions is $C_9^{\text{NP}} = -C_{10}^{\text{NP}} < 0$, with $C_9^{\text{NP}}$ large. This corresponds to the $(\bar{s}_L\gamma_\mu b_L)(\bar{\ell}_L\gamma^\mu\ell_L)$ operator of ref. [25].

In ref. [29], Glashow, Guadagnoli and Lane (GGL) stressed that the NP responsible for lepton flavor non-universality will generally also lead to lepton-flavor-violating (LFV) effects. To illustrate this, they proposed the following explanation of the $R_K$ puzzle. The NP is assumed to couple preferentially to the third generation with $(V-A)\times(V-A)$ form, giving rise to the operator

$$\frac{G}{\Lambda_{\text{NP}}^2}\left(\bar{b}_L'\gamma_\mu b_L'\right)\left(\bar{\tau}_L'\gamma^\mu\tau_L'\right) , \tag{1.4}$$

where $G = O(1)$, $G/\Lambda_{\text{NP}}^2 \ll G_F$, and the primed fields are the fermion eigenstates in the gauge basis. When one transforms to the mass basis, this generates the operator $(\bar{b}_L\gamma_\mu s_L)(\bar{\mu}_L\gamma^\mu\mu_L)$ that contributes to $\bar{b} \to \bar{s}\mu^+\mu^-$. The contribution to $\bar{b} \to \bar{s}e^+e^-$ is much smaller, leading to a violation of lepton flavor universality. GGL's point was that LFV decays, such as $B \to K\mu e$, $K\mu\tau$ and $B_s^0 \to \mu e$, $\mu\tau$, are also generated.

In ref. [30], it was pointed out that, assuming the scale of NP is much larger than the weak scale, the operator of eq. (1.4) should be made invariant under the full $\text{SU}(3)_C \times \text{SU}(2)_L \times \text{U}(1)_Y$ gauge group. There are two possibilities:

$$\begin{aligned} \mathcal{O}_1^{\text{NP}} &= \frac{G_1}{\Lambda_{\text{NP}}^2}\left(\bar{Q}_L'\gamma_\mu Q_L'\right)\left(\bar{L}_L'\gamma^\mu L_L'\right) , \\ \mathcal{O}_2^{\text{NP}} &= \frac{G_2}{\Lambda_{\text{NP}}^2}\left(\bar{Q}_L'\gamma_\mu\sigma^I Q_L'\right)\left(\bar{L}_L'\gamma^\mu\sigma^I L_L'\right) \\ &= \frac{G_2}{\Lambda_{\text{NP}}^2}\left[2\left(\bar{Q}_L'^i\gamma_\mu Q_L'^j\right)\left(\bar{L}_L'^j\gamma^\mu L_L'^i\right) - \left(\bar{Q}_L'\gamma_\mu Q_L'\right)\left(\bar{L}_L'\gamma^\mu L_L'\right)\right] , \end{aligned} \tag{1.5}$$

where $G_1$ and $G_2$ are both $O(1)$, and the $\sigma^I$ are the Pauli matrices. Here $Q' \equiv (t', b')^T$ and $L' \equiv (\nu_\tau', \tau')^T$. The key point is that $\mathcal{O}_2^{\text{NP}}$ contains both neutral-current (NC) and charged-current (CC) interactions. The NC and CC pieces can be used to respectively



JHEP01(2017)015

explain the $R_K$ and $R_{D^{(*)}}$ puzzles.[2] (Of course, while a common model of these anomalies is intriguing, it is also more constraining than separate explanations of the two puzzles.)

This method was explored in greater detail in ref. [44]. The starting point is the model-independent effective Lagrangian based on eq. (1.5):

$$\mathcal{L}_{\rm NP} = \frac{G_1}{\Lambda_{\rm NP}^2}\left(\bar{Q}'_L\gamma_\mu Q'_L\right)\left(\bar{L}'_L\gamma^\mu L'_L\right) + \frac{G_2}{\Lambda_{\rm NP}^2}\left(\bar{Q}'_L\gamma_\mu \sigma^I Q'_L\right)\left(\bar{L}'_L\gamma^\mu \sigma^I L'_L\right). \tag{1.6}$$

These operators are written in the gauge basis and involve only third-generation fermions. In transforming from the gauge basis to the mass basis, the left-handed down- and up-type quarks are operated upon by the matrices $D$ and $U$, respectively, where the Cabibbo-Kobayashi-Maskawa (CKM) matrix is $V_{CKM} = U^\dagger D$. The leptons are different: neglecting the neutrino masses, the left-handed charged and neutral leptons are both operated upon by the same matrix $L$. In ref. [44] it is assumed that the transformations $D$ and $L$ lead to mixing only between the second and third generations, so that they each depend on only one unknown theoretical parameter, respectively $\theta_D$ and $\theta_L$. In the mass basis, the above operators contribute to a variety of $B$ decays. Ref. [44] considers the following processes/observables: (i) $b \to s\ell^+\ell^-$ ($\ell = \mu,\, e$): $B \to K^*\mu^+\mu^-$, $B_s^0 \to \phi\mu^+\mu^-$, $R_K$, (ii) $b \to c\tau^-\bar{\nu}_\tau$: $R_{D^{(*)}}$, (iii) $b \to s\nu\bar{\nu}$: $B \to K^{(*)}\nu\bar{\nu}$ [45, 46]. The experimental measurements thus put constraints on the coefficients, which are all functions of $G_1$, $G_2$, $\theta_D$ and $\theta_L$. When all constraints are taken into account, it is found that the $R_K$ and $R_{D^{(*)}}$ puzzles can be simultaneously explained if $\theta_L$ is of the order of $\pi/16$ and $\theta_D$ is very small (less than $V_{cb}$). With these values for $\theta_L$ and $\theta_D$, one can make predictions for the rates of other (LFV) processes, and this is done for $B \to K^{(*)}\ell\ell'$ and $B_s^0 \to \ell\ell'$ ($\ell\ell' = \tau\mu, \tau e, \mu e$).

Finally, ref. [44] considers possible UV completions that can give rise to $\mathcal{O}_2^{\rm NP}$ [eq. (1.5)], that is required to explain both $R_K$ and $R_{D^{(*)}}$. Its coefficient $(G_2/\Lambda_{\rm NP}^2)$ suggests that this operator is generated by the tree-level exchange of a single particle. In this case, there are only four possibilities for the underlying NP model: (i) a vector boson ($VB$) that transforms as $(\mathbf{1},\mathbf{3},0)$ under $\mathrm{SU}(3)_C \times \mathrm{SU}(2)_L \times \mathrm{U}(1)_Y$, as in the SM, (ii) an $\mathrm{SU}(2)_L$-triplet scalar leptoquark ($S_3$) $[(\mathbf{3},\mathbf{3},-2/3)]$, (iii) an $\mathrm{SU}(2)_L$-singlet vector leptoquark ($U_1$) $[(\mathbf{3},\mathbf{1},4/3)]$, (iv) an $\mathrm{SU}(2)_L$-triplet vector leptoquark ($U_3$) $[(\mathbf{3},\mathbf{3},4/3)]$. The vector boson generates only $\mathcal{O}_2^{\rm NP}$, but the leptoquarks generate particular combinations of $\mathcal{O}_1^{\rm NP}$ and $\mathcal{O}_2^{\rm NP}$ [47]. It is shown that the combination of $\mathcal{O}_1^{\rm NP}$ and $\mathcal{O}_2^{\rm NP}$ generated by the $S_3$ and $U_3$ leptoquarks cannot simultaneously explain $R_K$ and $R_{D^{(*)}}$. The only possible UV completions are therefore the $VB$ and $U_1$ models.

But this now raises a question. If the NP responsible for the $R_K$ and $R_{D^{(*)}}$ puzzles leads to the effective Lagrangian of eq. (1.6), the underlying NP model is either $VB$ or $U_1$. But which is it? Short of actually producing a $W'/Z'$ or a leptoquark in an experiment, is there any way of distinguishing the two models? At first glance, the answer is no. After all, the two models lead to the same effective Lagrangian and so are "equivalent." However, this is not really true. To see this, one has to understand the difference between analyses

[2]Other analyses of the $R_{D^{(*)}}$ puzzle can be found in refs. [31–37]. Distributions in $\bar{B} \to D^{(*)}\tau^-\bar{\nu}_\tau$ decays can provide information on the type of new physics present in these decays [38–40]. Efforts to simultaneously explain multiple flavor anomalies can be found in refs. [41–43].



JHEP01(2017)015

based on an effective field theory (EFT) and those based on models. In an EFT analysis, one writes all effective operators of a given order; these are considered as independent. The effective Lagrangian of eq. (1.6) includes all four-fermion operators containing two quarks and two leptons. One can also write four-quark and four-lepton operators. But since these are uncorrelated with the operators with two quarks and two leptons, and since only processes of the type $q \to q'\ell\ell^{(\prime)}$ are studied, these other operators are uninteresting. But this does not hold in a model analysis. Concretely, while both $VB$ and $U_1$ models lead to operators with two quarks and two leptons, $VB$ also produces four-quark and four-lepton operators at tree level. In particular, it will contribute significantly to $B_s^0$-$\bar{B}_s^0$ mixing and the lepton-flavor-violating decay $\tau \to 3\mu$. These will lead to additional constraints on $\theta_D$ and $\theta_L$, respectively. Furthermore, while $VB$ contributes to $B \to K^{(*)}\nu\bar{\nu}$, $U_1$ does not. The bottom line is that the experimental constraints on the $VB$ model are more stringent than those on the $U_1$ model. Thus, the predictions for the rates of other processes can be very different in the two models, and this may allow us to distinguish them. It is this feature that is studied in the present paper.

We begin in section 2 by reviewing the method of ref. [44] for generating contributions to $R_K$ and $R_{D^{(*)}}$, as well as the NP models in which this can occur. These include the vector-boson model $VB$ and the $S_3$, $U_1$ and $U_3$ leptoquark models. The experimental measurements that constrain these models are described in section 3. These include not only processes involving $b \to s\ell^+\ell^-$, $b \to s\nu\bar{\nu}$ and $b \to c\tau^-\bar{\nu}$, but also $\tau \to \mu\phi$, $B_s^0$-$\bar{B}_s^0$ mixing and $\tau \to 3\mu$. These experimental constraints are applied to the models in section 4. As in ref. [44], we find that $S_3$ and $U_3$ are excluded, leaving only $VB$ and $U_1$. However, the constraints from $B_s^0$-$\bar{B}_s^0$ mixing and $\tau \to 3\mu$ are so stringent that the $VB$ model is only barely viable. In section 5 we examine the predictions of $VB$ and $U_1$ for other processes, to see if the two models can be distinguished. We find that, in fact, there are a number of different ways of doing this. Useful processes/observables include $\tau \to 3\mu$, $R_K$, and a previously overlooked lepton-flavor-violating decay, $\Upsilon \to \mu\tau$. We conclude in section 6.

## 2 Models

Including the generation indices $i, j, k, l$, the effective Lagrangian of eq. (1.6) can be written as

$$\mathcal{L}_{\rm NP} = \frac{G_1^{ijkl}}{\Lambda_{\rm NP}^2}\left(\bar{Q}_L^{(\prime)i}\gamma_\mu Q_L^{(\prime)j}\right)\left(\bar{L}_L^{(\prime)k}\gamma^\mu L_L^{(\prime)l}\right) + \frac{G_2^{ijkl}}{\Lambda_{\rm NP}^2}\left(\bar{Q}_L^{(\prime)i}\gamma_\mu \sigma^I Q_L^{(\prime)j}\right)\left(\bar{L}_L^{(\prime)k}\gamma^\mu \sigma^I L_L^{(\prime)l}\right). \tag{2.1}$$

This holds in both the gauge and mass bases. The gauge eigenstates, which involve only third-generation fermions, are indicated by primes on the spinors; the mass eigenstates have no primes. In transforming from the gauge basis to the mass basis, we have

$$u'_L = U u_L\,, \quad d'_L = D d_L\,, \quad \ell'_L = L\ell_L\,, \quad \nu'_L = L\nu_L\,, \tag{2.2}$$

where $U$, $D$ and $L$ are $3\times3$ unitary matrices and the spinors $u^{(\prime)}$, $d^{(\prime)}$, $\ell^{(\prime)}$ and $\nu^{(\prime)}$ include all three generations of fermions. The fact that the left-handed charged and neutral leptons are



JHEP01(2017)015

both operated upon by the same matrix $L$ is a result of neglecting the neutrino masses.[3] The CKM matrix is given by $V_{CKM} = U^\dagger D$. The assumption of ref. [44] is that the transformations $D$ and $L$ involve only the second and third generations:

$$D = \begin{pmatrix} 1 & 0 & 0 \\ 0 & \cos\theta_D & \sin\theta_D \\ 0 & -\sin\theta_D & \cos\theta_D \end{pmatrix} , \quad L = \begin{pmatrix} 1 & 0 & 0 \\ 0 & \cos\theta_L & \sin\theta_L \\ 0 & -\sin\theta_L & \cos\theta_L \end{pmatrix} . \tag{2.3}$$

Because of these transformations, for the down-type quarks and charged leptons, couplings involving the second generation (possibly flavor-changing) are possible in the mass basis. (For the up-type quarks, the first generation can also be involved.)

Specifically, in the mass basis we have

$$G_n^{ijkl} = g_n X^{ij} Y^{kl} , \tag{2.4}$$

where $X$ and $Y$ include the transformations from the gauge to the mass basis. The exact forms of these matrices depend on which four-fermion operator is used. For the decay $b \to s\ell^+\ell^-$ we have

$$\begin{aligned} X &= D^\dagger \begin{pmatrix} 0 & 0 & 0 \\ 0 & 0 & 0 \\ 0 & 0 & 1 \end{pmatrix} D = \begin{pmatrix} 0 & 0 & 0 \\ 0 & \sin^2\theta_D & -\sin\theta_D\cos\theta_D \\ 0 & -\sin\theta_D\cos\theta_D & \cos^2\theta_D \end{pmatrix} , \\ Y &= L^\dagger \begin{pmatrix} 0 & 0 & 0 \\ 0 & 0 & 0 \\ 0 & 0 & 1 \end{pmatrix} L = \begin{pmatrix} 0 & 0 & 0 \\ 0 & \sin^2\theta_L & -\sin\theta_L\cos\theta_L \\ 0 & -\sin\theta_L\cos\theta_L & \cos^2\theta_L \end{pmatrix} . \end{aligned} \tag{2.5}$$

If up-type quarks are involved in a process (such as $b \to c\tau^-\bar\nu$), one must include the transformation matrix $U$ [eq. (2.2)]. Because $V_{CKM} = U^\dagger D$, the amplitude will involve factors of $V_{CKM}$ in addition to $X$ and $Y$.

In terms of components, the effective Lagrangian is

$$\begin{aligned} \mathcal{L}_{\rm NP} = {} & \frac{\left(G_1^{ijkl} + G_2^{ijkl}\right)}{\Lambda_{\rm NP}^2} \left[\left(\bar u_L^i \gamma_\mu u_L^j\right)\left(\bar\nu_L^k \gamma^\mu \nu_L^l\right) + \left(\bar d_L^i \gamma_\mu d_L^j\right)\left(\bar\ell_L^k \gamma^\mu \ell_L^l\right)\right] \\ & + \frac{\left(G_1^{ijkl} - G_2^{ijkl}\right)}{\Lambda_{\rm NP}^2} \left[\left(\bar u_L^i \gamma_\mu u_L^j\right)\left(\bar\ell_L^k \gamma^\mu \ell_L^l\right) + \left(\bar d_L^i \gamma_\mu d_L^j\right)\left(\bar\nu_L^k \gamma^\mu \nu_L^l\right)\right] \\ & + 2\,\frac{G_2^{ijkl}}{\Lambda_{\rm NP}^2} \left[\left(\bar u_L^i \gamma_\mu d_L^j\right)\left(\bar\ell_L^k \gamma^\mu \nu_L^l\right) + \text{h.c.}\right] . \end{aligned} \tag{2.6}$$

[3] If neutrino masses are not neglected, the matrices $L$ and $N$ operate on the left-handed charged and neutral leptons, respectively, and the Pontecorvo-Maki-Nakagawa-Sakata (PMNS) matrix is $V_{PMNS} = N^\dagger L$. However, in processes such as $b \to c\tau^-\bar\nu_\tau$ and $b \to s\nu\bar\nu$, the final-state neutrinos are not detected, and so one must sum over all neutrinos. In this case, since $V_{PMNS}$ is unitary ($V_{PMNS}^\dagger V_{PMNS} = 1$), its effect on these processes vanishes.



JHEP01(2017)015

For the processes of interest, the NP contributions are

$$b \to s\mu^+\mu^- \,:\, \frac{(g_1+g_2)}{\Lambda^2_{\rm NP}} X^{23}Y^{22}\,(\bar{s}_L\gamma_\mu b_L)\,(\bar{\mu}_L\gamma^\mu\mu_L) + \text{h.c.}\,, \tag{2.7}$$

$$b \to s\nu\bar{\nu} \,:\, \frac{(g_1-g_2)}{\Lambda^2_{\rm NP}} X^{23}Y^{kl}\,(\bar{s}_L\gamma_\mu b_L)\left(\bar{\nu}^k_L\gamma^\mu\nu^l_L\right) + \text{h.c.} \quad \text{for } k,l=2,3\,, \tag{2.8}$$

$$b \to c\tau^-\bar{\nu} \,:\, \frac{2g_2}{\Lambda^2_{\rm NP}}\left[(V_{CKM}X)^{23}Y^{3l}\,(\bar{c}_L\gamma_\mu b_L)\left(\bar{\tau}_L\gamma^\mu\nu^l_L\right) + \text{h.c.}\right] \quad \text{for } l=2,3\,. \tag{2.9}$$

From these expressions, we see that there is no NP contribution to $b \to s\nu\bar{\nu}$ ($b \to s\mu^+\mu^-$) if $g_1 = g_2$ ($g_1 = -g_2$).

In the above, the NP is described in effective field theory language, as in ref. [44]. However, we are interested in explicitly studying the models that can lead to this EFT. There are two categories of NP models, those with new vector bosons, and those that involve leptoquarks. Below we summarize the features of the various models.

### 2.1 SM-like vector bosons

This model contains vector bosons ($VB$s) that transform as $(\mathbf{1},\mathbf{3},0)$ under $\mathrm{SU}(3)_C \times \mathrm{SU}(2)_L \times \mathrm{U}(1)_Y$, as in the SM. We refer to the $VB$s as $V = W'$, $Z'$.

In the gauge basis, the Lagrangian describing the couplings of the $VB$s to left-handed third-generation fermions is

$$\Delta\mathcal{L}_V = g^{33}_{qV}\left(\overline{Q}'_{L3}\;\gamma^\mu\sigma^I\;Q'_{L3}\right)V^I_\mu \;+\; g^{33}_{\ell V}\left(\overline{L}'_{L3}\;\gamma^\mu\sigma^I\;L'_{L3}\right)V^I_\mu\,, \tag{2.10}$$

where $\sigma^I$ ($I=1,2,3$) are the Pauli matrices. Once the heavy $VB$ is integrated out, we obtain the following effective Lagrangian, relevant for $b \to s\ell^+\ell^-$, $b \to c\tau^-\bar{\nu}$ and $b \to s\nu\bar{\nu}$ decays:

$$\mathcal{L}^{\rm eff}_V = -\frac{g^{33}_{qV}g^{33}_{\ell V}}{m^2_V}\left(\overline{Q}'_{L3}\gamma^\mu\sigma^I\;Q'_{L3}\right)\left(\overline{L}'_{L3}\gamma_\mu\sigma^I L'_{L3}\right). \tag{2.11}$$

Comparing this with eq. (2.1), we find

$$g_1 = 0\;, \qquad g_2 = -g^{33}_{qV}g^{33}_{\ell V}\,. \tag{2.12}$$

Note that $g_2$ can be either positive or negative in this model.

When one transforms to the mass basis, the $VB$s couple to other generations. The $Z'$ contributes at tree level to $b \to s\mu^+\mu^-$ and $b \to s\nu\bar{\nu}$; the $W'$ contributes at tree level to $b \to c\tau^-\bar{\nu}$. These contributions are given in eqs. (2.7)–(2.9) for the above values of $g_1$ and $g_2$.

The above processes all involve four-fermion operators that contain two quarks and two leptons. But $VB$ exchange also produces four-quark and four-lepton operators at tree level. In the gauge basis, the corresponding effective Lagrangian is

$$\begin{aligned}\mathcal{L}^{4Q,4L}_{\rm NP} = &-\frac{\left(g^{33}_{qV}\right)^2}{2m^2_V}\left(\overline{Q}'_{L3}\gamma^\mu\sigma^I Q'_{L3}\right)\left(\overline{Q}'_{L3}\gamma_\mu\sigma^I Q'_{L3}\right)\\ &-\frac{\left(g^{33}_{\ell V}\right)^2}{2m^2_V}\left(\overline{L}'_{L3}\gamma^\mu\sigma^I L'_{L3}\right)\left(\overline{L}'_{L3}\gamma_\mu\sigma^I L'_{L3}\right).\end{aligned} \tag{2.13}$$



JHEP01(2017)015

| Fierz Transformations |
|---|
| $(\overline{a}_L b^c_L)(\overline{c}^c_L d_L) = -\frac{1}{2}(\overline{a}_L \gamma^\mu d_L)(\overline{c}^c_L \gamma_\mu b^c_L)$ |
| $(\overline{a}_L \gamma^\mu b_L)(\overline{c}_L \gamma_\mu d_L) = (\overline{a}_L \gamma^\mu d_L)(\overline{c}_L \gamma_\mu b_L)$ |
| **Identities involving Pauli Matrices** |
| $\sigma^2_{ij}\sigma^2_{kl} = \frac{1}{2}\delta_{il}\delta_{kj} - \frac{1}{2}\sigma^I_{il}\cdot(\sigma^I)^T_{kj}$ |
| $\sigma^I_{ij}\sigma^2_{jk}\sigma^2_{lm}\sigma^I_{mn} = \frac{3}{2}\delta_{\text{in}}\delta_{lk} + \frac{1}{2}\sigma^I_{\text{in}}\cdot(\sigma^I)^T_{lk}$ |
| $\delta_{ij}\delta_{kl} = \frac{1}{2}\delta_{il}\delta_{kj} + \frac{1}{2}\sigma^I_{il}\cdot\sigma^I_{kj}$ |
| $\sigma^I_{ij}\sigma^I_{kl} = \frac{3}{2}\delta_{il}\delta_{kj} - \frac{1}{2}\sigma^I_{il}\cdot\sigma^I_{kj}$ |

**Table 1**. Fierz transformations and Pauli-matrix identities used in the analysis of LQ models.

In the mass basis, these contribute to processes such as $B^0_s$-$\bar{B}^0_s$ mixing and $\tau \to 3\mu$, and their measurements can be used to further constrain the $VB$ model.

There are a number of variants of the $VB$ model — for example, see refs. [48–52]. Note that some of these models address the $b \to s\mu^+\mu^-$ anomalies with a $Z'$, while others also try to explain the $R_{D^{(*)}}$ puzzle. In some models, new fermions are involved. This introduce additional parameters, which can lead to more flexibility in predictions.

### 2.2 Leptoquarks

In refs. [35, 53] it was shown that six different types of leptoquark (LQ) models can explain $R_{D^{(*)}}$. Of these, only four lead to four-fermion operators of the desired $(V-A)\times(V-A)$ form: (i) a scalar $\text{SU}(2)_L$ singlet $S_1$, (ii) a scalar $\text{SU}(2)_L$ triplet $S_3$, (iii) a vector $\text{SU}(2)_L$ singlet $U_1$, (iv) a vector $\text{SU}(2)_L$ triplet $U_3$. In general, tree-level LQ exchange generates $\mathcal{O}_1^{\text{NP}}$ and $\mathcal{O}_2^{\text{NP}}$ [47]. However, different models will produce different combinations of the two operators. Below, with the help of the identities in table 1, we determine these combinations for each of the four LQ models. That is, we derive the relation between $g_1$ and $g_2$, as well as the signs of these quantities.

Note that, unlike the $VB$ model, four-quark and four-lepton operators are not produced in LQ models at tree level.

#### 2.2.1 $\text{SU}(2)_L$-singlet scalar LQ ($S_1$)

$S_1$ is a scalar LQ that is an $\text{SU}(2)_L$ triplet (it transforms as $(\mathbf{3},\mathbf{1},-2/3)$ under $\text{SU}(3)_C \times \text{SU}(2)_L \times \text{U}(1)_Y$). In the gauge basis, the interaction Lagrangian for the $S_1$ LQ is given by [53]

$$\Delta\mathcal{L}_{S_1} = h^{33}_{S_1}\left(\overline{Q}'_{L3} i\sigma^2 L'^c_{L3}\right) S_1 + \text{h.c.}\,, \tag{2.14}$$



JHEP01(2017)015

where $\psi^c = C\bar{\psi}^T$ denotes a charge-conjugated fermion field. When the heavy LQ is integrated out, we obtain the following effective Lagrangian:

$$\begin{aligned}\mathcal{L}_{S_1}^{\text{eff}} &= \frac{\left|h_{S_1}^{33}\right|^2}{m_{S_1}^2}\left(\overline{Q}'_{L3i}\sigma^2_{ij}L'^c_{L3j}\right)\left(\overline{L}'^c_{L3k}\sigma^2_{kl}Q'_{L3l}\right) \\ &= \frac{\left|h_{S_1}^{33}\right|^2}{4m_{S_1}^2}\left[\left(\overline{Q}'_{L3}\gamma^\mu Q'_{L3}\right)\left(\overline{L}'_{L3}\gamma_\mu L'_{L3}\right) - \left(\overline{Q}'_{L3}\gamma^\mu\sigma^I Q'_{L3}\right)\left(\overline{L}'_{L3}\gamma_\mu\sigma^I L'_{L3}\right)\right].\end{aligned} \tag{2.15}$$

$\mathrm{SU}(2)_L$ indices have been inserted in the first line. In the second line, we have used relations from table 1 and then suppressed the indices. Comparing this with eq. (2.1), we find

$$g_1 = -g_2 = \frac{1}{4}\left|h_{S_1}^{33}\right|^2 > 0\,. \tag{2.16}$$

When one transforms to the mass basis, the $S_1$ LQ couples to other generations. However, because $g_1 = -g_2$, it does not contribute to $b \to s\mu^+\mu^-$ [eq. (2.7)] and hence cannot explain $R_K$. So this LQ model is not of interest to us.

#### 2.2.2 $\mathrm{SU}(2)_L$-triplet scalar LQ ($S_3$)

$S_3$ is a scalar LQ that is an $\mathrm{SU}(2)_L$ triplet (it transforms as $(\mathbf{3},\mathbf{3},-2/3)$). In the gauge basis, its interaction Lagrangian is given by [53]

$$\Delta\mathcal{L}_{S_3} = h_{S_3}^{33}\left(\overline{Q}'_{L3}\sigma^I i\sigma^2 L'^c_{L3}\right)S_3^I + \text{h.c.} \tag{2.17}$$

Integrating out the heavy LQ, we obtain the following effective Lagrangian:

$$\begin{aligned}\mathcal{L}_{S_3}^{\text{eff}} &= \frac{\left|h_{S_3}^{33}\right|^2}{m_{S_3}^2}\left(\overline{Q}'_{L3i}\sigma^I_{ij}\sigma^2_{jk}L'^c_{L3k}\right)\left(\overline{L}'^c_{L3l}\sigma^2_{lm}\sigma^I_{mn}Q'_{L3n}\right) \\ &= \frac{\left|h_{S_3}^{33}\right|^2}{4m_{S_3}^2}\left[3\left(\overline{Q}'_{L3}\gamma^\mu Q'_{L3}\right)\left(\overline{L}'_{L3}\gamma_\mu L'_{L3}\right) + \left(\overline{Q}'_{L3}\gamma^\mu\sigma^I Q'_{L3}\right)\left(\overline{L}'_{L3}\gamma_\mu\sigma^I L'_{L3}\right)\right].\end{aligned} \tag{2.18}$$

Comparing this with eq. (2.1), we find

$$g_1 = 3g_2 = \frac{3}{4}\left|h_{S_3}^{33}\right|^2 > 0\,. \tag{2.19}$$

When one transforms to the mass basis, the $S_3$ LQ couples to other generations. The components of the $\mathrm{SU}(2)_L$ triplet have $Q_{em} = \frac{2}{3}, -\frac{1}{3}, -\frac{4}{3}$. The $Q_{em} = \frac{2}{3}$ LQ contributes to $b \to s\ell^+\ell^-$ and $b \to c\tau^-\bar{\nu}$, while the $Q_{em} = -\frac{1}{3}$ LQ contributes to $b \to s\nu\bar{\nu}$. These contributions are given in eqs. (2.7)–(2.9) for the above values of $g_1$ and $g_2$.

The $S_3$ LQ has been studied in refs. [54, 55].

#### 2.2.3 $\mathrm{SU}(2)_L$-singlet vector LQ ($U_1$)

$U_1$ is a vector LQ that is an $\mathrm{SU}(2)_L$ singlet (it transforms as $(\mathbf{3},\mathbf{1},4/3)$). Its interaction Lagrangian is given in the gauge basis by [53]

$$\Delta\mathcal{L}_{U_1} = h_{U_1}^{33}\left(\overline{Q}'_{L3}\ \gamma^\mu\ L'_{L3}\right)U_{1\mu} + \text{h.c.} \tag{2.20}$$



JHEP01(2017)015

Integrating out the heavy LQ, and inserting $\mathrm{SU}(2)_L$ indices, we obtain the following effective Lagrangian:

$$\begin{aligned}\mathcal{L}^{\text{eff}}_{U_1} &= -\frac{\left|h^{33}_{U_1}\right|^2}{m^2_{U_1}}\left(\overline{Q}'_{L3i}\gamma^\mu\delta_{ij}\ L'_{L3j}\right)\left(\overline{L}'_{L3k}\gamma_\mu\delta_{kl}\ Q'_{L3l}\right) \\ &= -\frac{\left|h^{33}_{U_1}\right|^2}{2m^2_{U_1}}\left[\left(\overline{Q}'_{L3}\gamma^\mu Q'_{L3}\right)\left(\overline{L}'_{L3}\gamma^\mu L'_{L3}\right)+\left(\overline{Q}'_{L3}\gamma^\mu\sigma^I Q'_{L3}\right)\left(\overline{L}'_{L3}\gamma_\mu\sigma^I L'_{L3}\right)\right].\end{aligned} \tag{2.21}$$

Comparing this with eq. (2.1), we find

$$g_1 = g_2 = -\frac{1}{2}\left|h^{33}_{U_1}\right|^2 < 0\,. \tag{2.22}$$

In the mass basis, the $U_1$ LQ couples to other generations and contributes at tree level to $b\to s\mu^+\mu^-$ and $b\to c\tau^-\bar{\nu}$. These contributions are given in eqs. (2.7) and (2.9) for the above values of $g_1$ and $g_2$. However, because $g_1 = g_2$, there is no contribution to $b\to s\nu\bar{\nu}$.

The $U_1$ LQ has been studied in ref. [56].

#### 2.2.4 $\mathrm{SU}(2)_L$-triplet vector LQ ($U_3$)

The $U_3$ LQ is a vector that is an $\mathrm{SU}(2)_L$ triplet (it transforms as $(\mathbf{3},\mathbf{3},4/3)$). In the gauge basis, its interaction Lagrangian is given by [53]

$$\Delta\mathcal{L}_{U_3} = h^{33}_{U_3}\left(\overline{Q}'_{L3}\ \gamma^\mu\ \sigma^I L'_{L3}\right)U^I_{3\mu}\ +\ \text{h.c.} \tag{2.23}$$

When the heavy LQ is integrated out, the effective Lagrangian is

$$\begin{aligned}\mathcal{L}^{\text{eff}}_{U_3} &= -\frac{\left|h^{33}_{U_3}\right|^2}{m^2_{U_3}}\left(\overline{Q}'_{L3i}\gamma^\mu\sigma^I_{ij}\ L'_{L3j}\right)\left(\overline{L}'_{L3k}\gamma_\mu\sigma^I_{kl}\ Q'_{L3l}\right) \\ &= -\frac{\left|h^{33}_{U_3}\right|^2}{2m^2_{U_3}}\left[3\left(\overline{Q}'_{L3}\gamma^\mu Q'_{L3}\right)\left(\overline{L}'_{L3}\gamma^\mu L'_{L3}\right)-\left(\overline{Q}'_{L3}\gamma^\mu\sigma^I Q'_{L3}\right)\left(\overline{L}'_{L3}\gamma_\mu\sigma^I L'_{L3}\right)\right].\end{aligned} \tag{2.24}$$

Comparing this with eq. (2.1), we find

$$g_1 = -3g_2 = -\frac{3}{2}\left|h^{33}_{U_3}\right|^2 < 0\,. \tag{2.25}$$

In the mass basis, the $U_3$ LQ couples to other generations. The components of the $\mathrm{SU}(2)_L$ triplet have $Q_{em} = \frac{5}{3},\frac{2}{3},-\frac{1}{3}$. The $Q_{em} = \frac{2}{3}$ LQ contributes to $b\to s\ell^+\ell^-$ and $b\to c\tau^-\bar{\nu}$; the $Q_{em} = -\frac{1}{3}$ LQ contributes to $b\to s\nu\bar{\nu}$. These contributions are given in eqs. (2.7)–(2.9) for the above values of $g_1$ and $g_2$.

The $U_3$ LQ has been studied in refs. [57, 58].

### 2.3 Summary

We briefly recap the above results. We assume that the NP couples only to the third generation in the gauge basis, and that it produces four-fermion operators with a $(V-A)\times(V-A)$ structure. We find that there are four NP models that contribute to both $R_K$



JHEP01(2017)015

and $R_{D^{(*)}}$. There are two operators, $\mathcal{O}_1^{\rm NP}$ and $\mathcal{O}_2^{\rm NP}$, shown in eq. (2.1), whose coefficients are $g_1$ and $g_2$. The four models contribute differently to $\mathcal{O}_1^{\rm NP}$ and $\mathcal{O}_2^{\rm NP}$:

$$\begin{aligned}
VB &: g_1 = 0\,, \quad g_2 = -g_{qV}^{33} g_{\ell V}^{33}\ , \qquad g_2 \text{ can be positive or negative}\,,\\
S_3 &: g_1 = 3g_2 = \frac{3}{4}\left|h_{S_3}^{33}\right|^2 > 0\,,\\
U_1 &: g_1 = g_2 = -\frac{1}{2}\left|h_{U_1}^{33}\right|^2 < 0\,,\\
U_3 &: g_1 = -3g_2 = -\frac{3}{2}\left|h_{U_3}^{33}\right|^2 < 0\,.
\end{aligned} \tag{2.26}$$

In ref. [44], it is noted that $\lambda^{(3)}$ $(= g_2)$ is positive for the $S_3$ and $U_3$ models, but negative for $U_1$. This is confirmed by the above.

## 3 Constraints

When one transforms to the mass basis, two new parameters are introduced, $\theta_D$, $\theta_L$. The NP contributes to $b \to s\mu^+\mu^-$, $b \to s\nu\bar{\nu}$ and $b \to c\tau^-\bar{\nu}$. These contributions are given in eqs. (2.7)–(2.9); the coefficients are (different) functions of $g_1$, $g_2$, $\theta_D$, $\theta_L$. Another decay to which all four models contribute is $\tau \to \mu\phi$. In addition, the $VB$ model contributes to other processes, such as $B_s^0$-$\bar{B}_s^0$ mixing and $\tau \to 3\mu$. The experimental measurements of, or limits on, these processes provide constraints on the NP parameter space.

In order to compare models, we fix $\Lambda_{\rm NP} = 1\,\text{TeV}$ and assume a common value for $2g_{qV}^{33}g_{\ell V}^{33}$, $\left|h_{S_3}^{33}\right|^2$, $\left|h_{U_1}^{33}\right|^2$ and $\left|h_{U_3}^{33}\right|^2$. We apply all the experimental constraints to establish the allowed region in the $(\theta_D,\ \theta_L)$ parameter space. If there is no region in which all constraints overlap, the model is excluded. For the models that are retained, we predict the rates for other processes based on the allowed region in parameter space. Since this region can be different for different models, it may be possible to distinguish them.

### 3.1 $b \to s\ell^+\ell^-$, $b \to s\nu\bar{\nu}$, $b \to c\tau^-\bar{\nu}$

The effective Hamiltonians for $b \to s\ell^+\ell^-$, $b \to s\nu\bar{\nu}$ and $b \to c\tau^-\bar{\nu}$ are

$$\begin{aligned}
H_{\rm eff}\left(b \to s\ell_i\bar{\ell}_j\right) = &-\frac{\alpha G_F}{\sqrt{2}\pi} V_{tb}V_{ts}^* \Big[C_9^{ij}\ \left(\bar{s}_L\gamma^\mu b_L\right)\left(\bar{\ell}_i\gamma_\mu\ell_j\right)\\
&+ C_{10}^{ij}\ \left(\bar{s}_L\gamma^\mu b_L\right)\left(\bar{\ell}_i\gamma_\mu\gamma^5\ell_j\right)\Big]\,,
\end{aligned} \tag{3.1}$$

$$H_{\rm eff}\left(b \to s\nu_i\bar{\nu}_j\right) = -\frac{\alpha G_F}{\sqrt{2}\pi} V_{tb}V_{ts}^*\, C_L^{ij}\ \left(\bar{s}_L\gamma^\mu b_L\right)\left(\bar{\nu}_i\gamma_\mu(1-\gamma^5)\nu_j\right)\,, \tag{3.2}$$

$$H_{\rm eff}\left(b \to c\ell_i\bar{\nu}_j\right) = \frac{4G_F}{\sqrt{2}} V_{cb}C_V^{ij}\left(\bar{c}_L\gamma^\mu b_L\right)\left(\bar{\ell}_{iL}\gamma_\mu\nu_{jL}\right)\,, \tag{3.3}$$

where the Wilson coefficients include both the SM and NP contributions: $C_X = C_X(\text{SM}) + C_X(\text{NP})$. Comparing with eqs. (2.7)–(2.9) (and recalling that $\mathcal{L}_{\rm NP}$ and $H_{\rm eff}$ have opposite

signs), we have

$$C_9^{ij}(\mathrm{NP}) = -C_{10}^{ij}(\mathrm{NP}) = \frac{\pi}{\sqrt{2}\alpha G_F V_{tb}V_{ts}^*}\frac{(g_1+g_2)}{\Lambda_{\mathrm{NP}}^2}X^{23}Y^{ij}\,, \tag{3.4}$$

$$C_L^{ij}(\mathrm{NP}) = \frac{\pi}{\sqrt{2}\alpha G_F V_{tb}V_{ts}^*}\frac{(g_1-g_2)}{\Lambda_{\mathrm{NP}}^2}X^{23}Y^{ij}\,, \tag{3.5}$$

$$C_V^{ij}(\mathrm{NP}) = -\frac{1}{2\sqrt{2}G_F V_{cb}}\frac{2g_2}{\Lambda_{\mathrm{NP}}^2}\left(V_{cs}X^{23}+V_{cb}X^{33}\right)Y^{ij}\,. \tag{3.6}$$

In the following subsections we examine the experimentally-preferred values of the above quantities.

#### 3.1.1 $C_9^{\mu\mu}(\mathrm{NP}) = -C_{10}^{\mu\mu}(\mathrm{NP})$

A global analysis of the $b \to s\ell^+\ell^-$ anomalies was recently performed in ref. [10]. The fit included data on $B \to K^{(*)}\mu^+\mu^-$, $B \to K^{(*)}e^+e^-$, $B_s^0 \to \phi\mu^+\mu^-$, $B \to X_s\mu^+\mu^-$, $b \to s\gamma$ and $B_s^0 \to \mu^+\mu^-$. It was found that there is a significant disagreement with the SM, possibly as large as $4\sigma$, and that it can be explained if there is NP in $b \to s\mu^+\mu^-$. There are four possible explanations, each having roughly equal goodness-of-fits: (i) $C_9^{\mu\mu}(\mathrm{NP}) < 0$, (ii) $C_9^{\mu\mu}(\mathrm{NP}) = -C_{10}^{\mu\mu}(\mathrm{NP}) < 0$, (iii) $C_9^{\mu\mu}(\mathrm{NP}) = -C_9^{\prime\mu\mu}(\mathrm{NP}) < 0$, and (iv) $C_9^{\mu\mu}(\mathrm{NP}) = -C_{10}^{\mu\mu}(\mathrm{NP}) = -C_9^{\prime\mu\mu}(\mathrm{NP}) = -C_{10}^{\prime\mu\mu}(\mathrm{NP}) < 0$. Of these, it is solution (ii) that interests us. According to the fit, the allowed $3\sigma$ range for the Wilson coefficients is

$$-1.13 \le C_9^{\mu\mu}(\mathrm{NP}) = -C_{10}^{\mu\mu}(\mathrm{NP}) \le -0.21\,. \tag{3.7}$$

Note that the above range of the NP contribution is consistent with the $R_K$ anomaly: the central value of $R_K^{\mathrm{expt}}$ can be explained with $C_9^{\mu\mu}(\mathrm{NP}) \simeq -0.55$.

#### 3.1.2 $C_L^{ij}(\mathrm{NP})$

$C_L^{ij}(\mathrm{NP})$ can be constrained by the existing data of $\bar{B} \to K\nu\bar{\nu}$ and $\bar{B} \to K^*\nu\bar{\nu}$ decays. The BaBar and Belle Collaborations give the following 90% C.L. upper limits [45, 46]:

$$\begin{aligned}
\mathcal{B}\left(B^+ \to K^+\nu\bar{\nu}\right) &\le 1.7\times10^{-5}\,,\\
\mathcal{B}\left(B^+ \to K^{*+}\nu\bar{\nu}\right) &\le 4.0\times10^{-5}\,,\\
\mathcal{B}\left(B^0 \to K^{*0}\nu\bar{\nu}\right) &\le 5.5\times10^{-5}\,.
\end{aligned} \tag{3.8}$$

In ref. [59], these are compared with the SM predictions

$$\begin{aligned}
\mathcal{B}_K^{\mathrm{SM}} &\equiv \mathcal{B}\left(B \to K\nu\bar{\nu}\right)_{\mathrm{SM}} = (3.98 \pm 0.43 \pm 0.19)\times10^{-6}\,,\\
\mathcal{B}_{K^*}^{\mathrm{SM}} &\equiv \mathcal{B}\left(B \to K^*\nu\bar{\nu}\right)_{\mathrm{SM}} = (9.19 \pm 0.86 \pm 0.50)\times10^{-6}\,.
\end{aligned} \tag{3.9}$$

Taking into account the theoretical uncertainties [59], the 90% C.L. upper bounds on the NP contributions are

$$\frac{\mathcal{B}_K^{\mathrm{SM+NP}}}{\mathcal{B}_K^{\mathrm{SM}}} \le 4.8\ , \qquad \frac{\mathcal{B}_{K^*}^{\mathrm{SM+NP}}}{\mathcal{B}_{K^*}^{\mathrm{SM}}} \le 4.9\,. \tag{3.10}$$



JHEP01(2017)015

We have

$$\frac{\mathcal{B}_K^{\rm SM+NP}}{\mathcal{B}_K^{\rm SM}} = \frac{\mathcal{B}_{K^*}^{\rm SM+NP}}{\mathcal{B}_{K^*}^{\rm SM}} = \frac{1}{3|C_L^{\rm SM}|^2}\left(3|C_L^{\rm SM}|^2 + 2C_L^{\rm SM}\sum_{i=1}^{3}{\rm Re}[C_L^{ii}({\rm NP})] + \sum_{i,j=1}^{3}|C_L^{ij}({\rm NP})|^2\right), \tag{3.11}$$

where $C_L^{\rm SM} \simeq -1.47/\sin^2\theta_W \simeq -6.36$ ($\theta_W$ is the Weinberg angle). The bound on NP therefore becomes

$$-13\sum_{i=1}^{3}{\rm Re}[C_L^{ii}({\rm NP})] + \sum_{i,j=1}^{3}|C_L^{ij}({\rm NP})|^2 \leq 473\,. \tag{3.12}$$

A constraint on the NP contribution can also be obtained from the inclusive decay. The ALEPH Collaboration gives the 90% C.L. upper limit as $\mathcal{B}(B\to X_s\nu\bar{\nu}) \leq 6.4\times10^{-4}$ [60]. However, this implies $\mathcal{B}_{X_s}^{\rm SM+NP}/\mathcal{B}_{X_s}^{\rm SM} \leq 22$, which is a weaker constraint than that from the exclusive decays.

### 3.1.3 $C_V^{\ell\nu}({\rm NP})$

The constraint on $C_V^{ij}$ can be obtained from the comparison of the measurements of the ratios $R_{D^{(*)}} \equiv \mathcal{B}(\bar{B}\to D^{(*)}\tau^-\bar{\nu}_\tau)/\mathcal{B}(\bar{B}\to D^{(*)}\ell^-\bar{\nu}_\ell)$ ($\ell = e,\mu$) with their SM expectations. This is shown in eq. (1.2), and leads to the $3\sigma$ bounds

$$0.79 \leq R_D^{\rm ratio} \leq 1.79\ , \qquad 1.02 \leq R_{D^*}^{\rm ratio} \leq 1.53\,, \tag{3.13}$$

where

$$R_D^{\rm ratio} = R_{D^*}^{\rm ratio} = \frac{2\left(\left|1+C_V^{\tau\nu_\tau}({\rm NP})\right|^2 + \sum_{j=1,2}\left|C_V^{\tau\nu_j}({\rm NP})\right|^2\right)}{1+\left|1+C_V^{\mu\nu_\mu}({\rm NP})\right|^2 + \sum_{j=1,3}\left|C_V^{\mu\nu_j}({\rm NP})\right|^2}\,. \tag{3.14}$$

Here we have assumed $C_V^{e\nu_j}({\rm NP}) = 0$.

## 3.2 $\tau\to\mu\phi$

The NP effective Lagrangian of eq. (2.6) generates the process $\tau\to\mu s\bar{s}$:

$$\mathcal{L}_{\rm eff} = \frac{g_1+g_2}{\Lambda_{\rm NP}^2}X^{22}Y^{23}\left(\bar{s}_L\gamma^\mu s_L\right)\left(\bar{\tau}_L\gamma_\mu\mu_L\right)\,, \tag{3.15}$$

which will lead to $\tau\to\mu\phi$ and $\tau\to\mu\eta^{(\prime)}$. Writing the hadronic currents as

$$\langle 0|\bar{s}\gamma^\mu s|\phi\rangle = f_\phi m_\phi\epsilon_\phi^\mu\,, \quad \langle 0|\bar{s}\gamma^\mu s|\eta^{(\prime)}\rangle = if_{\eta^{(\prime)}}p_{\eta^{(\prime)}}^\mu\,, \tag{3.16}$$

the branching ratios (neglecting the mass of the muon) are given by

$$\begin{aligned}\mathcal{B}(\tau\to\mu\phi) &= \frac{f_\phi^2 m_\tau^3\tau_\tau}{128\pi\Lambda_{\rm NP}^4}|\kappa|^2\left(1-\eta_\phi^2\right)^2\left(1+2\eta_\phi^2\right)\,,\\ \mathcal{B}(\tau\to\mu\eta^{(\prime)}) &= \frac{f_{\eta^{(\prime)}}^2 m_\tau^3\tau_\tau}{128\pi\Lambda_{\rm NP}^4}|\kappa|^2\left(1-\eta_{\eta^{(\prime)}}^2\right)\,,\end{aligned} \tag{3.17}$$



JHEP01(2017)015

where $\kappa = (g_1 + g_2)X^{22}Y^{23}$, $\eta_\phi \equiv m_\phi/m_\tau$ and $\eta_\eta^{(\prime)} \equiv m_\eta^{(\prime)}/m_\tau$ . Thus we obtain the following ratio:

$$\frac{\mathcal{B}\left(\tau \to \mu\eta^{(\prime)}\right)}{\mathcal{B}(\tau \to \mu\phi)} = \frac{f_{\eta^{(\prime)}}^2}{f_\phi^2} \cdot \frac{1 - \eta_{\eta^{(\prime)}}^2}{\left(1 - \eta_\phi^2\right)^2 \left(1 + 2\eta_\phi^2\right)} \,. \tag{3.18}$$

We may use the following expression to estimate $f_\phi^2$:

$$f_\phi^2 = \frac{27 m_\phi \Gamma_\phi \mathcal{B}(\phi \to \mu^+\mu^-)}{4\pi\alpha_{\rm em}^2} \,. \tag{3.19}$$

Taking the values for $m_\phi$, $m_\tau$, $\tau_\tau$, $\Gamma_\phi$ and $\mathcal{B}(\phi \to \mu^+\mu^-)$ from ref. [61], this yields $f_\phi \approx 225$ MeV. For the $\eta^{(\prime)}$ decay constant we get (using $f_\pi = 130\,\text{MeV}$, $f_1 \sim 1.1 f_\pi$, $f_8 \sim 1.3 f_\pi$ [62] , and $\theta = 19.5^\circ$ [63])

$$\begin{aligned} f_\eta &= -\frac{f_\pi}{\sqrt{3}} \left( \sqrt{2}\cos\theta \frac{f_8}{f_\pi} + \sin\theta \frac{f_1}{f_\pi} \right) \simeq -157.63 \text{ MeV} \,, \\ f_{\eta'} &= \frac{f_\pi}{\sqrt{3}} \left( \cos\theta \frac{f_1}{f_\pi} - \sqrt{2}\sin\theta \frac{f_8}{f_\pi} \right) \simeq 31.76 \text{ MeV} \,. \end{aligned} \tag{3.20}$$

Using these we obtain

$$\frac{\mathcal{B}(\tau \to \mu\eta)}{\mathcal{B}(\tau \to \mu\phi)} \sim 0.60 \,, \quad \frac{\mathcal{B}(\tau \to \mu\eta')}{\mathcal{B}(\tau \to \mu\phi)} \sim 1.9 \times 10^{-2} \,. \tag{3.21}$$

The current 90% C.L. limits on these branching ratios are [61]

$$\begin{aligned} \mathcal{B}(\tau \to \mu\eta) &< 6.5 \times 10^{-8} \,, \\ \mathcal{B}(\tau \to \mu\eta') &< 1.3 \times 10^{-7} \,, \\ \mathcal{B}(\tau \to \mu\phi) &< 8.4 \times 10^{-8} \,. \end{aligned} \tag{3.22}$$

Of these decays, $\tau \to \mu\eta'$ is the least constraining. And since $\tau \to \mu\phi$ and $\tau \to \mu\eta$ are of the same order, we will use $\tau \to \mu\phi$ to constrain the coupling $\kappa$. Using $\mathcal{B}(\tau \to \mu\phi) < 8.4 \times 10^{-8}$ [64] and $\Lambda_{\rm NP} = 1\,\text{TeV}$, we obtain the constraint

$$|\kappa| < 0.019 \,. \tag{3.23}$$

### 3.3 $B_s^0$-$\bar{B}_s^0$ mixing

As noted in section 2.1, the $VB$ model also generates four-quark operators at tree level. In the mass basis, the operator of eq. (2.13) includes

$$\frac{(g_{qV}^{33})^2}{2m_V^2} \sin^2\theta_D \cos^2\theta_D \left(\bar{s}_L\gamma^\mu b_L\right)\left(\bar{s}_L\gamma_\mu b_L\right) \,. \tag{3.24}$$

This generates a contribution to $B_s^0$-$\bar{B}_s^0$ mixing. In the SM, the same operator is produced via a box diagram. Here we have

$$N C_{VLL}^{\rm SM} \left(\bar{s}_L\gamma^\mu b_L\right)\left(\bar{s}_L\gamma_\mu b_L\right) , \tag{3.25}$$



JHEP01(2017)015

where

$$N = \frac{G_F^2 m_W^2}{16\pi^2} (V_{tb}V_{ts}^*)^2 \sim 10^{-11}\,\text{GeV}^{-2}\,,$$
$$C_{VLL}^{\text{SM}} = \eta_{B_s} x_t \left[1 + \frac{9}{1-x_t} - \frac{6}{(1-x_t)^2} - \frac{6x_t^2 \ln x_t}{(1-x_t)^3}\right]. \tag{3.26}$$

In the above, $x_t \equiv m_t^2/m_W^2$ and $\eta_{B_s} = 0.551$ is the QCD correction [65]. The SM and NP contributions can be combined. We define

$$NC_{VLL} \equiv NC_{VLL}^{\text{SM}} + \frac{\left(g_{qV}^{33}\right)^2}{2m_V^2} \sin^2\theta_D \cos^2\theta_D\,. \tag{3.27}$$

The mass difference in the $B_s$ system is then given by

$$\Delta M_s = \frac{2}{3} m_{B_s} f_{B_s}^2 \hat{B}_{B_s} |NC_{VLL}|\,. \tag{3.28}$$

Taking $f_{B_s}\sqrt{\hat{B}_{B_s}} = (266 \pm 18)\,\text{MeV}$ [66, 67], $V_{tb}V_{ts}^* = -0.0405 \pm 0.0012$ [61, 68], and $\overline{m}_t = 160\,\text{GeV}$ [61, 69], we find the SM prediction

$$\Delta M_s^{\text{SM}} = (17.4 \pm 2.6)\ \text{ps}^{-1}\,. \tag{3.29}$$

This is to be compared with the experimental measurement [70]

$$\Delta M_s = (17.757 \pm 0.021)\ \text{ps}^{-1}\,. \tag{3.30}$$

As we will see in the next section, the constraint on the $VB$ model from $B_s^0$-$\bar{B}_s^0$ mixing is extremely stringent.

### 3.4 $\tau \to 3\mu$

Finally, the $VB$ model also produces four-lepton operators at tree level. In the mass basis, the Lagrangian of eq. (2.13) includes the operator

$$-\frac{(g_{\ell V}^{33})^2}{2m_V^2} \sin^3\theta_L \cos\theta_L \left(\bar{\mu}_L \gamma^\mu \tau_L\right)\left(\bar{\mu}_L \gamma_\mu \mu_L\right), \tag{3.31}$$

which generates the decay $\tau \to 3\mu$. As this is a lepton-flavor-violating decay, it can arise only due to NP. The decay rate for $\tau \to 3\mu$ is then given by

$$\mathcal{B}\left(\tau^- \to \mu^-\mu^+\mu^-\right) = X \frac{\left(g_{\ell V}^{33}\right)^4}{16 m_V^4} \frac{m_\tau^5 \tau_\tau}{192\pi^3} \sin^6\theta_L \cos^2\theta_L\,, \tag{3.32}$$

where $X$ is a suppression factor due to the non-zero muon mass. In terms of $\eta_\mu = m_\mu/m_\tau$, it is given by

$$X = 12 \int_{4\eta_\mu^2}^{(1-\eta_\mu)^2} \frac{dx}{\sqrt{x}} \left(x - 2\eta_\mu^2\right)\left(1 + \eta_\mu^2 - x\right) \sqrt{\left(x - 4\eta_\mu^2\right)\left(1 - 2\left(x + \eta_\mu^2\right) + \left(x + \eta_\mu^2\right)^2\right)}$$
$$\approx 0.94\,. \tag{3.33}$$

At present, the branching ratio for $\tau^- \to \mu^-\mu^+\mu^-$ has only an experimental upper bound [71]:

$$\mathcal{B}\left(\tau^- \to \mu^-\mu^+\mu^-\right) < 2.1 \times 10^{-8} \text{ at } 90\% \text{ C.L.} \tag{3.34}$$

This then puts a constraint on $\theta_L$ in the $VB$ model, which, as we will see in the next section, is quite strong.

## 4 Models: allowed parameter space

Taking into account all the experimental constraints described in section 3, we find the allowed parameter space in the four NP models. We assume $\Lambda_{\rm NP} = 1\,\text{TeV}$, and take the third-generation coupling to be $2g_{qV}^{33}g_{\ell V}^{33} = \left|h_{U_1}^{33}\right|^2 = \left|h_{U_3}^{33}\right|^2 = \left|h_{S_3}^{33}\right|^2 = 1$. For the $VB$ model, we take $g_{qV}^{33} = g_{\ell V}^{33}$. (In the next section we vary $g_{qV}^{33}$ and $g_{\ell V}^{33}$.) In figure 1, the constraints in the $(\theta_L, \theta_D)$ plane are shown for the $VB$, $U_1$, $U_3$ and $S_3$ models. These are presented only for $\theta_L \geq 0$; the space is symmetric under $\theta_L \to -\theta_L$.

For all four models, the flavor anomalies $R_D$, $R_{D^*}$ and $R_K$ can be explained in the shaded regions colored in pink, red and blue, respectively. The gray shaded region is allowed from $\bar{B} \to K^{(*)}\nu\bar{\nu}$ at 90% C.L. The region bounded by the green lines is consistent with the 90% C.L. upper limit on the branching ratio of $\tau \to \mu\phi$. For the $VB$ model, there are additional constraints coming from $B_s^0$-$\bar{B}_s^0$ mixing and $\tau \to 3\mu$. For the $\tau \to 3\mu$ constraint, the region to the left of the cyan line is allowed. The $B_s^0$-$\bar{B}_s^0$ mixing constraint is shown in the orange region, which is extremely narrow near $\theta_D = 0, \pi/2$.

Based on this figure, one can make two observations:

- There are only two regions in parameter space where the constraints from $R_D$, $R_{D^*}$, $R_K$ and $\bar{B} \to K^{(*)}\nu\bar{\nu}$ (if applicable) might overlap. These are roughly around $\pi/16 \lesssim \theta_L \lesssim \pi/8$, with $\theta_D$ near 0 (region 1) or $\pi/2$ (region 2). However, the additional constraint from $\tau \to \phi\mu$ distinguishes the two regions. That is, while region 1 satisfies the $\tau \to \phi\mu$ constraint, region 2 does not, and is therefore excluded. Henceforth, we focus only on region 1.

- For the $VB$ model, the constraint from $B_s^0$-$\bar{B}_s^0$ mixing has the same shape as that from $\bar{B} \to K^{(*)}\nu\bar{\nu}$. They are both independent of $\theta_L$, and so bound only $\theta_D$. However, we see that the $B_s^0$-$\bar{B}_s^0$ mixing constraint is much more stringent than that from $\bar{B} \to K^{(*)}\nu\bar{\nu}$. For $g_{qV}^{33} = g_{\ell V}^{33} = 1/\sqrt{2}$, one has $|\theta_D| \ll 1$, so that it is somewhat difficult from this figure to determine if this region is consistent with the others.

In order to obtain more information, in figure 2, we show the constraints in region 1 of the $(\theta_L, \theta_D)$ plane for the $VB$, $S_3$, $U_1$, and $U_3$ models. In the figures, we indicate the values of the contours for the flavor anomalies, that is, $R_X^{\rm NP+SM}/R_X^{\rm SM}$ for $X = K$ and $D^{(*)}$. From this figure, we can see that

- For the $S_3$ model, the $R_{D^*}$ region does not overlap with the $R_K$ or $\bar{B} \to K^{(*)}\nu\bar{\nu}$ regions. And for the $U_3$ model, the $R_{D^*}$ and $\bar{B} \to K^{(*)}\nu\bar{\nu}$ regions do not overlap. Therefore, $S_3$ and $U_3$ with the flavor mixing structure of eq. (2.5) are excluded.[4]

[4] A different type of the mixing for the $U_3$ LQ is discussed in ref. [57].



JHEP01(2017)015

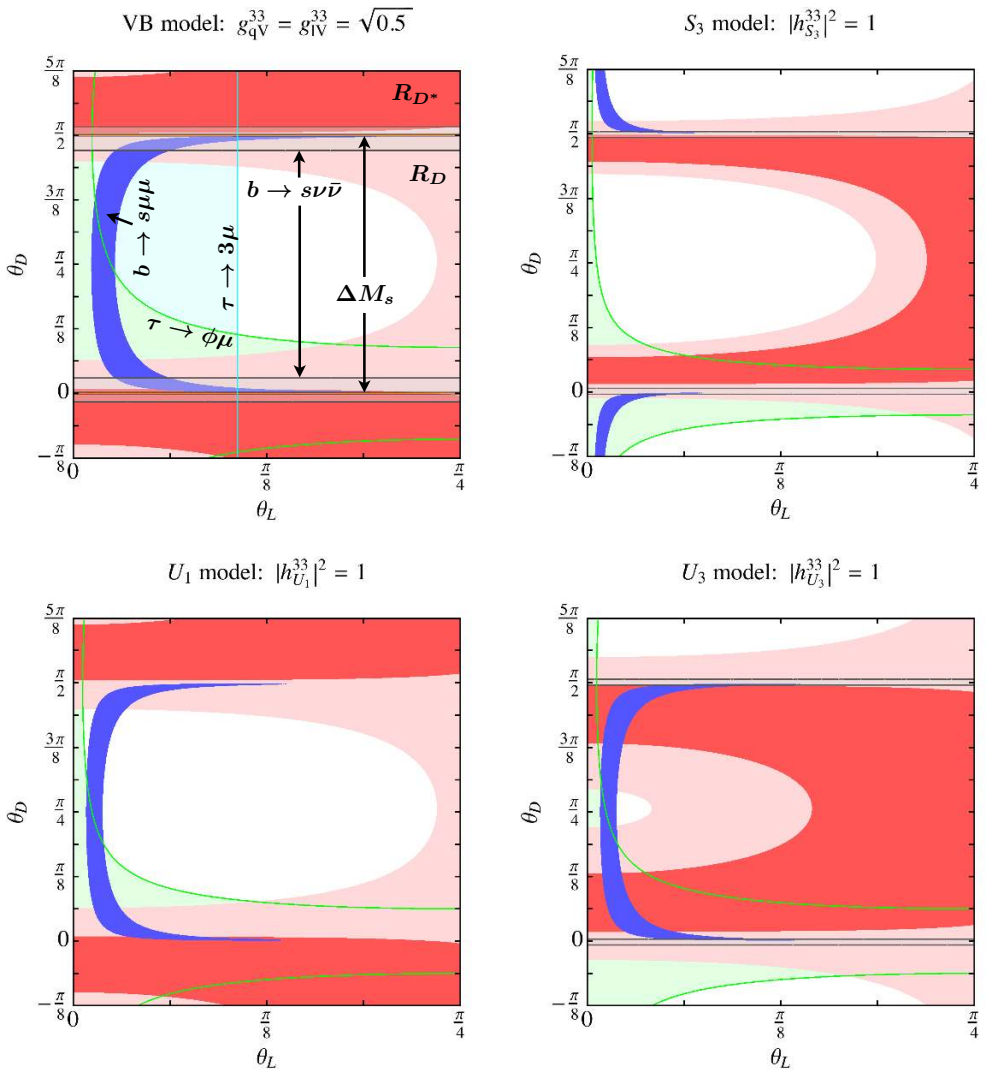


**Figure 1**. Allowed regions in the $(\theta_L, \theta_D)$ plane for the $VB$, $S_3$, $U_1$, and $U_3$ models. We have fixed the NP scale as $\Lambda_{\rm NP} = 1\,\text{TeV}$. In each model, the third-generation coupling is taken as $2g_{qV}^{33}g_{\ell V}^{33} = \left|h_{U_1}^{33}\right|^2 = \left|h_{U_3}^{33}\right|^2 = \left|h_{S_3}^{33}\right|^2 = 1$. The $R_D$, $R_{D^*}$ and $R_K$ (along with the $b \to s\ell^+\ell^-$ data) anomalies can be explained in the shaded regions colored in pink, red, and blue, respectively. The regions bounded by the gray, green, cyan, and orange lines are allowed from the measurements of $b \to s\nu\bar{\nu}$, $\tau \to \mu\phi$, $\tau \to 3\mu$, and $\Delta M_s$, respectively. The last two observables are applicable only in the $VB$ model.

- For the $U_1$ model, if $\theta_D \leq 0.028$, there is a region where all the constraints overlap, and so this model is allowed. On the other hand, the $VB$ model is on the edge of exclusion — the boundaries of the $\Delta M_s$, $b \to s\mu\mu$, and $\tau \to 3\mu$ constraints are touching, but just barely. This also implies that the $VB$ model only allows limited values of these observables. From this figure we see that $\tau \to 3\mu$ is a critical process for the $VB$ model. Therefore, in addition to the 90% C.L. upper bound on $\mathcal{B}(\tau^- \to \mu^-\mu^+\mu^-)$ from eq. (3.34) shown in the figure (solid cyan line), we superpose an estimated $3\sigma$ upper limit on this branching ratio (dashed cyan line).



JHEP01(2017)015

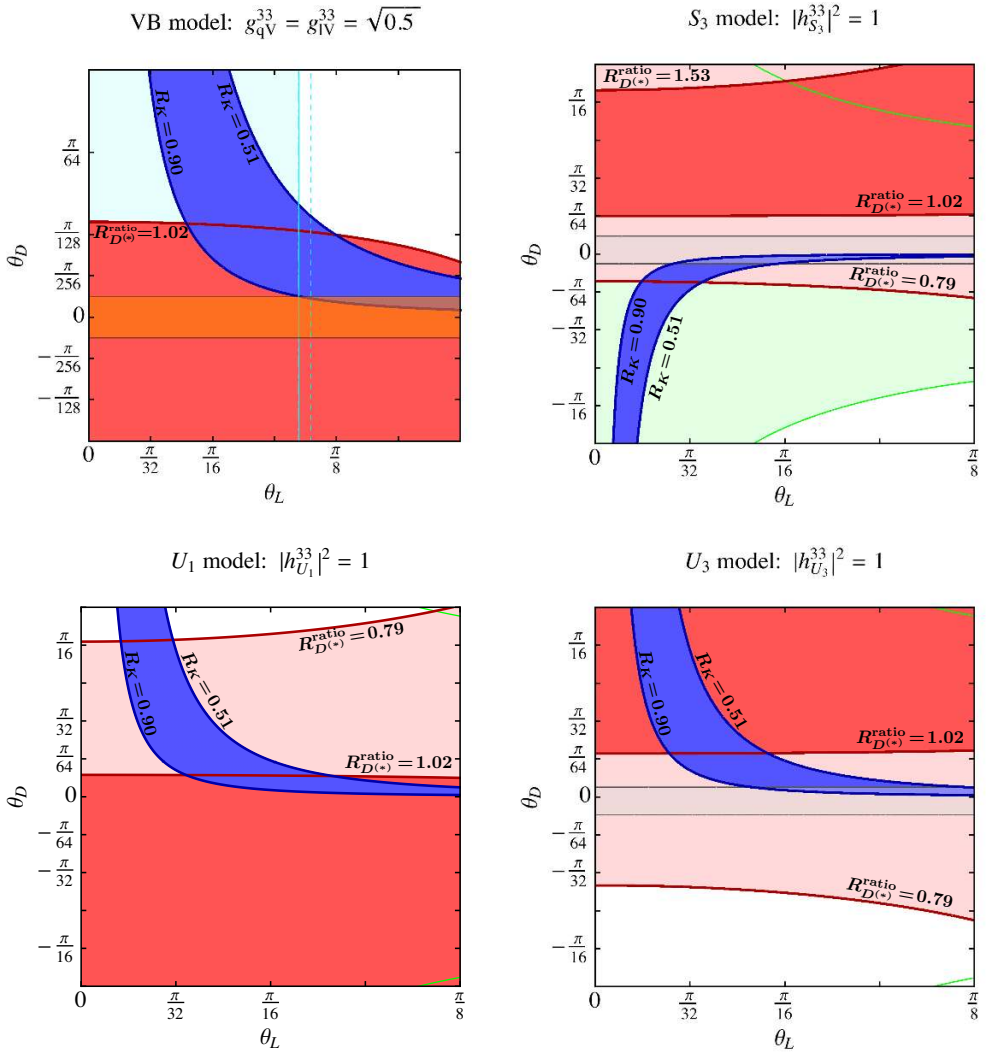


**Figure 2**. Magnified figures of figure 1. The color legends are the same as the previous figures. The values of the contours for $R_X^{\rm NP+SM}/R_X^{\rm SM}$ ($X = K, D, D^*$) are indicated. The $R_D$ constraint (in pink) is satisfied for the entire region of the plot in $VB$ and hence omitted.

- Comparing the $VB$ and $U_1$ models, the constraints from the flavor anomalies ($R_K$, $R_{D^{(*)}}$) are similar (for $\theta_D$ near 0). But the additional constraints from $\Delta M_s$ and $\tau \to 3\mu$ put $VB$ on the verge of exclusion. The limited amount of parameter space available to $VB$ increases its predictive power. Specifically, while the allowed region for the $U_1$ model includes $0.11 \leq \theta_L \leq 0.73$ and $0.001 \leq \theta_D \leq 0.028$, for the $VB$ model $(\theta_L, \theta_D)$ is limited to be $\simeq (0.333, 0.006)$.

The $VB$ and $U_1$ models are therefore the candidates to simultaneously explain the $R_K$ and $R_{D^{(*)}}$ puzzles in the case where the NP couples predominantly to the third-generation fermions.



JHEP01(2017)015

## 5 Predictions

We have now established that the $VB$ and $U_1$ models are candidates to explain the present discrepancies with the SM in $b \to s\mu^+\mu^-$, $R_{D^{(*)}}$ and $R_K$. The main question we wish to address in this paper is: is there any way of distinguishing the two models? There are two handles that can potentially accomplish this. First, the $VB$ model contributes to four-lepton and four-quark operators, and hence to processes such as $\tau \to 3\mu$ and $B_s^0$-$\bar{B}_s^0$ mixing, while the $U_1$ model does not.[5] Second, due to additional constraints, the allowed region in $(\theta_L, \theta_D)$ space is essentially a single point for $VB$, while it is much larger for $U_1$. Below we explore the predictions of the two models for various processes. As we will see, it is potentially possible to distinguish the $VB$ and $U_1$ models.

### 5.1 Processes

#### 5.1.1 $R_{D^{(*)}}$

The $3\sigma$ allowed ranges of $R_{D^{(*)}}^{\text{ratio}}$ are given in eq. (3.13). At present, large deviations from the SM are allowed (up to 79% and 53% for $R_D$ and $R_{D^*}$, respectively). On the other hand, from figure 2, we see that the $VB$ and $U_1$ models are allowed only if $\theta_D$ is very small. This means that such large deviations in $R_{D^{(*)}}$ from the SM are not favored, as these are inconsistent with the $R_K$ anomaly. The models predict

$$\begin{aligned} VB \quad &: \quad R_{D^{(*)}}^{\text{ratio}} \simeq 1.04\,, \\ U_1 \quad &: \quad 1.02 \le R_{D^{(*)}}^{\text{ratio}} \le 1.05\,. \end{aligned} \tag{5.1}$$

Thus, even if $R_{D^{(*)}}$ is measured with greater precision, it will probably not be possible to distinguish the $VB$ and $U_1$ models. However, if the measurements confirm large deviations from the SM, both models will be ruled out.

#### 5.1.2 $R_K$

The situation is different for $R_K$. Using eq. (1.1), its allowed $3\sigma$ range is $0.498 \le R_K \le 1.036$. The models predict [73]

$$\begin{aligned} VB \quad &: \quad R_K \simeq 0.90\,, \\ U_1 \quad &: \quad 0.51 \le R_K \le 0.90\,. \end{aligned} \tag{5.2}$$

We therefore see that the $U_1$ model can accomodate smaller values of $R_K$ than can the $VB$ model. This is due to the fact that its allowed $(\theta_L, \theta_D)$ region includes larger values of $\theta_L$. Thus, if future measurements of $R_K$ find it to be less than 0.90 at higher than 90% C.L., this would point clearly to $U_1$ (and exclude $VB$).

[5] In this paper we perform the analysis at tree level. Radiative corrections to four-lepton operators have been considered in ref. [72] within an EFT framework. However, as with all EFT analyses, the results do not necessarily apply to all models. To obtain the proper result, a more complete analysis must be done within each individual model.



JHEP01(2017)015

#### 5.1.3 $\tau \to 3\mu$

This decay is particularly interesting because only the $VB$ model contributes to it. The present experimental bound is $\mathcal{B}(\tau^- \to \mu^-\mu^+\mu^-) < 2.1 \times 10^{-8}$ at 90% C.L. [eq. (3.34)]. Belle II expects to reduce this limit to $< 10^{-10}$ [74]. The reach of LHCb is somewhat weaker, $< 10^{-9}$ [75].

Now, the amplitude for $\tau \to 3\mu$ depends only on $\theta_L$ [eq. (3.31)]. In figure 2, we see that the allowed value of $\theta_L$ corresponds to the present experimental bound. That is, $VB$ predicts

$$\mathcal{B}(\tau^- \to \mu^-\mu^+\mu^-) \simeq 2.1 \times 10^{-8}\,. \tag{5.3}$$

Thus, the $VB$ model predicts that $\tau \to 3\mu$ should be observed at both LHCb and Belle II. This is a smoking-gun signal for the model.

#### 5.1.4 $B \to K^{(*)}\mu\tau$

The BaBar Collaboration obtained an experimental bound of $\mathcal{B}(B^+ \to K^+\mu^\pm\tau^\mp) < 4.8 \times 10^{-5}$ at 90% C.L. [76]. Belle II will collect 100 times more data than BaBar, and this will allow it to measure $\mathcal{B}(B^+ \to K^+\mu^\pm\tau^\mp)$ to a level of $5 \times 10^{-7}$ [77].

The models predict [73]

$$\begin{aligned} VB \quad &: \quad \mathcal{B}\left(B \to K^{(*)}\mu\tau\right) \simeq 4.0 \times 10^{-10}\,, \\ U_1 \quad &: \quad 6.8 \times 10^{-11} \le \mathcal{B}\left(B \to K^{(*)}\mu\tau\right) \le 2.1 \times 10^{-8}\,. \end{aligned} \tag{5.4}$$

Neither model can produce $\mathcal{B}(B \to K^{(*)}\mu\tau)$ sufficiently large that it can be observed at Belle II.

#### 5.1.5 $B \to K^{(*)}\tau^+\tau^-$

The BaBar Collaboration recently put a limit of $\mathcal{B}(B^+ \to K^+\tau^+\tau^-) < 2.25 \times 10^{-3}$ at 90% C.L. [78]. Belle II will be able to improve on this, but because there are two $\tau$'s in the final state, the expected reach is only $\sim 2 \times 10^{-4}$ [77].

To measure and calculate the branching ratio of $B \to K^{(*)}\tau^+\tau^-$, we need to deal with charmonium resonances. In analogy with $B \to K^{(*)}\mu^+\mu^-$, we take $q^2 > 15\,\text{GeV}^2$ for integration and obtain the partial branching ratio by using `flavio` [73]:

$$\begin{aligned} VB \quad &: \quad \mathcal{B}\left(B \to K^{(*)}\tau^+\tau^-\right) \simeq 4.4 \times 10^{-8}\,, \\ U_1 \quad &: \quad 7.6 \times 10^{-10} \le \mathcal{B}\left(B \to K^{(*)}\tau^+\tau^-\right) \le 1.5 \times 10^{-6}\,. \end{aligned} \tag{5.5}$$

The values of $\mathcal{B}(B \to K^{(*)}\tau^+\tau^-)$ possible in both models are at least two orders of magnitude smaller than the estimated reach of Belle II. This decay can therefore not be used as a signal of the $VB$ and/or $U_1$ models.



JHEP01(2017)015

#### 5.1.6 $B_s^0 \to \mu\tau$, $B_s^0 \to \tau^+\tau^-$

At present, LHCb is working on measuring these two decays, which are difficult due to the presence of $\tau$'s in the final state. However, no estimates of the reach are available [79]. (At Belle II, a rough estimate for $B_s^0 \to \tau^+\tau^-$ could be $\sim 2 \times 10^{-3}$ with $50\,\text{ab}^{-1}$ of data, obtained by rescaling the present data at Belle.)

For $B_s^0 \to \mu\tau$, the models predict

$$\begin{aligned} VB \quad &: \quad \mathcal{B}\left(B_s^0 \to \mu\tau\right) \simeq 6.7 \times 10^{-9}\,, \\ U_1 \quad &: \quad 1.1 \times 10^{-9} \leq \mathcal{B}\left(B_s^0 \to \mu\tau\right) \leq 3.6 \times 10^{-7}\,, \end{aligned} \tag{5.6}$$

while for $B_s^0 \to \tau^+\tau^-$ we have

$$\begin{aligned} VB \quad &: \quad \mathcal{B}\left(B_s^0 \to \tau^+\tau^-\right) \simeq 2.4 \times 10^{-7}\,, \\ U_1 \quad &: \quad 5.8 \times 10^{-18} \leq \mathcal{B}\left(B_s^0 \to \tau^+\tau^-\right) \leq 6.7 \times 10^{-6}\,. \end{aligned} \tag{5.7}$$

For $B_s^0 \to \mu\tau$, if the branching ratio were measured to be between $6.7 \times 10^{-9}$ and $3.6 \times 10^{-7}$, this would point to the $U_1$ model. However, it is unlikely that such a small branching ratio is measurable. Similarly, if $\mathcal{B}(B_s^0 \to \tau^+\tau^-)$ were found to be in the range $2.4 \times 10^{-7}$–$6.7 \times 10^{-6}$, this would indicate $U_1$. However, here too it is not clear that such a small branching ratio is measurable.

#### 5.1.7 $\Upsilon \to \mu\tau$

Finally, we turn to $\Upsilon \to \mu\tau$. This lepton-flavor-violating decay has been overlooked in previous analyses, but it is potentially an important process to consider.[6] At the fermion level, this decay is $b\bar{b} \to \mu\tau$, and it can receive contributions from both the $VB$ and $U_1$ models. Note that this process has a pattern of mixing different from the above processes, and thus the models provide unique predictions.

In the past, the BaBar [81] and CLEO [82] Collaborations have studied lepton flavor violation in narrow $\Upsilon(nS)(n = 1, 2, 3)$ decays. The strongest limits come from BaBar [81], which put an upper limit on $\mathcal{B}(\Upsilon(2S, 3S) \to \mu\tau)$ of a few times $10^{-6}$. This was obtained using $13.6\,\text{fb}^{-1}$ and $26.8\,\text{fb}^{-1}$ of the BaBar dataset on the $\Upsilon(2S)$ and $\Upsilon(3S)$, respectively. Belle II is expected to collect a few hundred $\text{fb}^{-1}$ of data on the $\Upsilon(3S)$ [77]. A precise estimate of the sensitivity to $\Upsilon(3S) \to \mu\tau$ will require a dedicated study. However, given the order-of-magnitude increase in luminosity at Belle II compared to BaBar, we expect roughly an order-of-magnitude improvement in the sensitivity. That is, a reach of about $10^{-7}$ for $\mathcal{B}(\Upsilon(3S) \to \mu\tau)$ at Belle II is not unreasonable. These decays may also be studied at LHCb, but we are not aware of the LHCb reach for these processes.

In the SM, the LFV decay $\Upsilon(nS) \to \ell^-\ell'^+$, where $\ell$ and $\ell'$ represent leptons of different flavor, is highly suppressed. On the other hand, in the $VB$ and $U_1$ models, $\Upsilon(nS) \to \mu^-\tau^+$ receives significant contributions. Assuming the NP is purely left-handed, the decay rate for this process is given by

$$\Gamma\left(\Upsilon(nS) \to \mu^-\tau^+\right) = \frac{m^3_{\Upsilon(nS)} f^2_{\Upsilon(nS)}}{48\pi}\left(1 - \eta_\tau^2\right)\left(2 - \eta_\tau^2 - \eta_\tau^4\right)|\kappa|^2\,, \tag{5.8}$$

[6] Quark flavor violating quarkonium decays were considered in ref. [80].



JHEP01(2017)015

where $\eta_\tau = m_\tau/m_{\Upsilon(nS)}$ and $\kappa$ contains the coupling corresponding to the transition $b\bar{b} \to \tau\mu$. In the $VB$ and $U_1$ models we have

$$\kappa = -\frac{g_1+g_2}{2\Lambda_{\rm NP}^2} X^{33}Y^{32} = \frac{g_1+g_2}{2\Lambda_{\rm NP}^2}\cos^2\theta_D \cos\theta_L \sin\theta_L\,. \tag{5.9}$$

The decay constant $f_{\Upsilon(nS)}$ can be found using the electromagnetic decay $\Upsilon(nS) \to \ell^-\ell^+$, which is unaffected by NP. Its decay rate can be expressed as

$$\Gamma\left(\Upsilon(nS) \to \ell^-\ell^+\right) = \frac{4\pi\alpha^2}{27}\frac{f_{\Upsilon(nS)}^2}{m_{\Upsilon(nS)}}\left(1+2\eta_{\ell(nS)}^2\right)\sqrt{1-4\eta_{\ell(nS)}^2}\,, \tag{5.10}$$

where $\eta_{\ell(nS)} = m_\ell/m_{\Upsilon(nS)}$.

We may now combine eqs. (5.8), (5.9) and (5.10) to get predictions for the branching ratio of $\Upsilon(nS) \to \mu\tau$ in the $VB$ and $U_1$ models. These are

$$\begin{aligned}
VB \quad &: \quad \mathcal{B}(\Upsilon(1S) \to \mu\tau) \simeq 2.3\times10^{-9}\,,\\
&\qquad\ \ \mathcal{B}(\Upsilon(2S) \to \mu\tau) \simeq 2.3\times10^{-9}\,,\\
&\qquad\ \ \mathcal{B}(\Upsilon(3S) \to \mu\tau) \simeq 3.0\times10^{-9}\,,\\
U_1 \quad &: \quad 1.1\times10^{-9} \le \mathcal{B}(\Upsilon(1S) \to \mu\tau) \le 2.4\times10^{-8}\,,\\
&\qquad\ \ 1.2\times10^{-9} \le \mathcal{B}(\Upsilon(2S) \to \mu\tau) \le 2.4\times10^{-8}\,,\\
&\qquad\ \ 1.5\times10^{-9} \le \mathcal{B}(\Upsilon(3S) \to \mu\tau) \le 3.2\times10^{-8}\,.
\end{aligned} \tag{5.11}$$

The $VB$ model predicts a branching ratio of $O(10^{-9})$, while it can be $O(10^{-8})$ in the $U_1$ model. Therefore this mode can potentially allow us to distinguish between the two models. However, even the upper limit predicted by the $U_1$ model seems to be out of reach of Belle II, according to our estimate of its reach. On the other hand, perhaps Belle II or LHCb will in fact be sensitive to branching ratios of $O(10^{-8})$. Or perhaps the NP coupling is bigger than we have assumed (see section 5.2 below), resulting in larger branching ratios. The point is that $\Upsilon \to \mu\tau$ decays may provide us with valuable information in identifying the lepton-flavor-violating NP.

#### 5.1.8 Summary

There are therefore three observables that can distinguish the $VB$ and $U_1$ models:

1. $\tau \to 3\mu$: $VB$ predicts $\mathcal{B}(\tau^- \to \mu^-\mu^+\mu^-) \simeq 2.1\times10^{-8}$, its present upper limit ($U_1$ does not contribute to the decay). This implies that the LFV decay $\tau \to 3\mu$, which is absent in the SM, should be observed at both LHCb and Belle II. This is therefore a smoking-gun signal: it can occur only in the $VB$ model, and if the decay is not seen, the model would be ruled out.

2. $R_K$: the current $3\sigma$ range for $R_K$ is $0.498 \le R_K \le 1.036$. The $U_1$ model can accomodate smaller values of $R_K$, while the $VB$ model cannot. Specifically, if future measurements of $R_K$ find it to be less than 0.90 at higher than 90% C.L., this would point to $U_1$ (and exclude $VB$).



JHEP01(2017)015

3. $\Upsilon \to \mu\tau$: to date, the LFV decay $\Upsilon \to \mu\tau$ has been overlooked as a test of NP models in $B$ decays. Within the $VB$ model, $\mathcal{B}(\Upsilon(nS) \to \mu\tau)$ is a few times $10^{-9}$, but in the $U_1$ model, it can reach a few times $10^{-8}$. Belle II should be able to measure $\mathcal{B}(\Upsilon(3S) \to \mu\tau)$ down to $\sim 10^{-7}$. However, this is only a very rough estimate — a detailed study is needed for a precise determination of the reach. It may be that, in fact, Belle II (or LHCb) will be able to observe branching ratios of $O(10^{-8})$. And if the decay $\Upsilon \to \mu\tau$ is observed, this will suggest the $U_1$ model.

There are five other observables that receive contributions in the $VB$ and $U_1$ models: $R_{D^{(*)}}$, $B \to K^{(*)}\mu\tau$, $B \to K^{(*)}\tau^+\tau^-$, $B_s^0 \to \mu\tau$, $B_s^0 \to \tau^+\tau^-$. However, either these observables cannot distinguish the two models, or, if they can, the predicted branching ratios fall below the expected reach of Belle II and LHCb.

### 5.2 Varying the couplings

Now, the results of the previous subsection have been found assuming that $2\, g_{qV}^{33} g_{\ell V}^{33} = \left|h_{U_1}^{33}\right|^2 = 1$. However, there is nothing special about this value of the square of the coupling (henceforth denoted coupling$^2$). This then raises the question: if the coupling$^2$ is allowed to take different values, how do the results of section 5.1 change? This is examined in this subsection.

For each new value of the coupling$^2$, one must redo the analysis of section 4, to determine the region in $(\theta_L, \theta_D)$ parameter space allowed by the various experimental constraints. That is, figures of the type in figure 2 are produced. The following results are found:

- For the $S_3$ and $U_3$ models, it is found that the $R_{D^*}$ and $\bar{B} \to K^{(*)}\nu\bar{\nu}$ regions do not overlap, and this is independent of the value of coupling$^2$. $S_3$ and $U_3$ are therefore excluded.

- For the $VB$ model, the constraints essentially come from three observables:

  1. $B_s^0$-$\bar{B}_s^0$ mixing ($\Delta M_s$): puts an upper bound on $g_{qV}^{33} \sin\theta_D \cos\theta_D$ [eq. (3.24)].
  2. $\tau \to 3\mu$: puts an upper bound on $(g_{\ell V}^{33})^2 \sin^3\theta_L \cos\theta_L$ [eq. (3.31)].
  3. $b \to s\mu^+\mu^-$ ($C_9^{\mu\mu}$(NP)): puts a lower bound on $(g_{qV}^{33} \sin\theta_D \cos\theta_D)(g_{\ell V}^{33} \sin^2\theta_L)$. (There is also an upper bound, but this is not relevant for the $VB$ model.)

  These three constraints overlap at basically a single point in the parameter space. However, one still has the freedom to relabel this point by adjusting the values of $g_{qV}^{33}$, $g_{\ell V}^{33}$, $\theta_L$ and $\theta_D$. For example, in the previous section we had $g_{qV}^{33} = g_{\ell V}^{33} = \sqrt{0.5}$, $(\theta_L, \theta_D) = (0.333, 0.006)$. However, two other possibilities are $g_{qV}^{33} = \sqrt{0.5}/0.8$, $g_{\ell V}^{33} = 0.8\sqrt{0.5}$, $(\theta_L, \theta_D) = (0.392, 0.005)$ and $g_{qV}^{33} = \sqrt{0.28}/1.2$, $g_{\ell V}^{33} = 1.2\sqrt{0.28}$, $(\theta_L, \theta_D) = (0.360, 0.009)$. But the key point is that, in both of these cases, the predictions for other processes are little changed from those in section 5.1.

- The $U_1$ model is viable only if $\left|h_{U_1}^{33}\right|^2 \geq 0.5$. Values of the coupling$^2$ larger than 5 are allowed, see figure 3.



JHEP01(2017)015

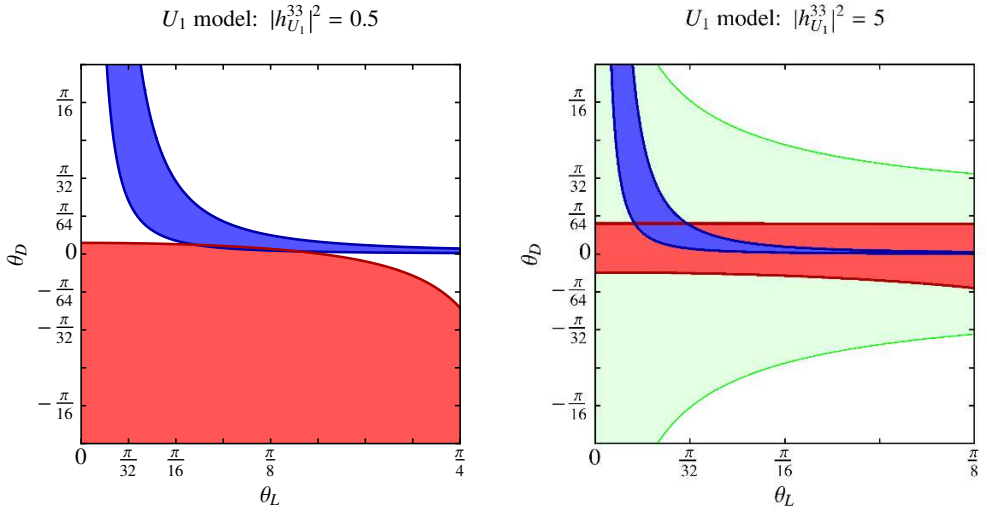


**Figure 3**. Figure 2 for the $U_1$ model, but with $\left|h^{33}_{U_1}\right|^2 = 0.5$ (left) or $\left|h^{33}_{U_1}\right|^2 = 5$ (right). Left: the blue ($R_K$) and red ($R_{D^*}$) regions barely overlap, so this is the minimum value of the coupling$^2$ for which $U_1$ is viable. Right: the regions overlap, so $U_1$ is viable for $\left|h^{33}_{U_1}\right|^2 = 5$ (as well as for larger values of the coupling$^2$).

In fact, we do have some information about the value of the coupling$^2$. One can set limits on coupling$^2/\Lambda^2_{\rm NP}$ from direct searches, assuming a certain mode of production for the new mediator states. Following ref. [83], using the $b\bar{b} \to \tau\bar{\tau}$ process mediated by $s$- or $t$-channel vector-boson or leptoquark exchange, one can get the following rough upper bounds: $|g^{33}_{qV} g^{33}_{\ell V}|_{\rm max}/\Lambda^2_{\rm NP} \sim 3\,{\rm TeV}^{-2}$ for the $VB$ model and $\left|h^{33}_{U_1}\right|^2_{\rm max}/\Lambda^2_{\rm NP} \sim 5\,{\rm TeV}^{-2}$ for the $U_1$ model. That is, for $\Lambda_{\rm NP} = 1\,{\rm TeV}$, $g^{33}_{qV} g^{33}_{\ell V} \leq 3$ and $\left|h^{33}_{U_1}\right|^2 \leq 5$.[7]

In light of these results, we rederive the predictions of the $U_1$ model for the various observables, allowing $0.5 \leq \left|h^{33}_{U_1}\right|^2 \leq 5$. For comparison, we include the $VB$ predictions from section 5.1. We find

1. $R_{D^{(*)}}$:

$$\begin{aligned} VB \quad &: \quad R^{\rm ratio}_{D^{(*)}} \simeq 1.04\,, \\ U_1 \quad &: \quad 1.02 \leq R^{\rm ratio}_{D^{(*)}} \leq 1.29\,. \end{aligned} \tag{5.12}$$

   For coupling$^2 = 1$, we found that, for both models, large deviations in $R_{D^{(*)}}$ from the SM are not favored, so it is not possible to distinguish the $VB$ and $U_1$ models using $R_{D^{(*)}}$. From the above numbers, we see that, when the coupling$^2$ is allowed to vary, this no longer holds. If it is found that $1.04 < R_{D^{(*)}} \leq 1.29$, this will indicate $U_1$.

[7] To be precise, the bound given in ref. [83] should be applied as $g^{33}_{qV} g^{33}_{\ell V} \cos^2\theta_D \cos^2\theta_L \leq 3$ and $\left|h^{33}_{U_1} \cos\theta_D \cos\theta_L\right|^2 \leq 5$ (for $\Lambda_{\rm NP} = 1\,{\rm TeV}$). The down-sector mixing, which reduces the rate of $b\bar{b}$ pair production, is negligible since $\theta_D \ll 1$ for the present case. As for the lepton mixing, it can at most reduce the decay rate into $\tau\bar{\tau}$ by 15% (for $\theta_L \leq \pi/8$). Here we (conservatively) ignore this effect, resulting in a slightly more stringent constraint on coupling$^2$, as shown in the main text.



JHEP01(2017)015

2. $R_K$:

$$\begin{aligned} VB &: R_K \simeq 0.90\,, \\ U_1 &: 0.51 \leq R_K \leq 0.90\,. \end{aligned} \tag{5.13}$$

The result is as before: if future measurements find $0.51 \leq R_K < 0.90$, this would point clearly to $U_1$ (and exclude $VB$).

3. $B \to K^{(*)}\mu\tau$:

$$\begin{aligned} VB &: \mathcal{B}\left(B \to K^{(*)}\mu\tau\right) \simeq 4.0 \times 10^{-10}\,, \\ U_1 &: \mathcal{B}\left(B \to K^{(*)}\mu\tau\right)|_{\max} = 1.6 \times 10^{-7}\,. \end{aligned} \tag{5.14}$$

When the coupling[2] is allowed to vary, the value of $\mathcal{B}(B \to K^{(*)}\mu\tau)|_{\max}$ predicted by the $U_1$ model is larger than in section 5.1. Unfortunately, it is still below the reach of Belle II (which is $5 \times 10^{-7}$ [77]).

4. $B \to K^{(*)}\tau^+\tau^-$:

$$\begin{aligned} VB &: \mathcal{B}\left(B \to K^{(*)}\tau^+\tau^-\right) \simeq 4.4 \times 10^{-8}\,, \\ U_1 &: \mathcal{B}\left(B \to K^{(*)}\tau^+\tau^-\right)|_{\max} = 1.1 \times 10^{-4}\,. \end{aligned} \tag{5.15}$$

Here too, when the coupling[2] is allowed to vary, we find that the value of $\mathcal{B}(B \to K^{(*)}\tau^+\tau^-)|_{\max}$ for the $U_1$ model is increased over that in section 5.1. It may just be attainable at Belle II (its reach is $\sim 2 \times 10^{-4}$ [77]). Thus, $B \to K^{(*)}\tau^+\tau^-$ could perhaps be used to distinguish the two models.

5. $B_s^0 \to \mu\tau$:

$$\begin{aligned} VB &: \mathcal{B}\left(B_s^0 \to \mu\tau\right) \simeq 6.7 \times 10^{-9}\,, \\ U_1 &: \mathcal{B}\left(B_s^0 \to \mu\tau\right)|_{\max} = 2.8 \times 10^{-6}\,. \end{aligned} \tag{5.16}$$

Once again, the value of $\mathcal{B}(B_s^0 \to \mu\tau)|_{\max}$ for the $U_1$ model is larger than that in section 5.1. However, we cannot evaluate whether this decay can be used to distinguish the two models as we do not know the reach of LHCb or Belle II for $B_s^0 \to \mu\tau$.

6. $B_s^0 \to \tau^+\tau^-$

$$\begin{aligned} VB &: \mathcal{B}\left(B_s^0 \to \tau^+\tau^-\right) \simeq 2.4 \times 10^{-7}\,, \\ U_1 &: \mathcal{B}\left(B_s^0 \to \tau^+\tau^-\right)|_{\max} = 5.4 \times 10^{-4}\,. \end{aligned} \tag{5.17}$$

The value of $\mathcal{B}(B_s^0 \to \tau^+\tau^-)|_{\max}$ for the $U_1$ model is larger than before. However, we cannot evaluate whether this decay can be used to distinguish the two models as we do not know the reach of LHCb or Belle II for $B_s^0 \to \tau^+\tau^-$.



JHEP01(2017)015

7. $\Upsilon(3S) \to \mu\tau$:

$$\begin{aligned} VB \qquad & \mathcal{B}(\Upsilon(3S) \to \mu\tau) \simeq 3.0 \times 10^{-9}\,, \\ U_1 \quad : \quad & \mathcal{B}(\Upsilon(3S) \to \mu\tau)|_{\rm max} = 8.0 \times 10^{-7}\,. \end{aligned} \tag{5.18}$$

Previously, we made a rough estimate that Belle II should be able to measure $\mathcal{B}(\Upsilon(3S) \to \mu\tau)$ down to $\sim 10^{-7}$. We speculated that perhaps Belle II could do better than this (and noted that a precise determination of the reach can only be obtained through a detailed study). However, the above predicted values of $\mathcal{B}(\Upsilon(3S) \to \mu\tau)|_{\rm max}$ show that, even with our rough estimate, the $U_1$ model can lead to rates for $\Upsilon(3S) \to \mu\tau$ that are easily observable at Belle II. If this decay were seen, it would exclude $VB$ and point to $U_1$. This demonstrates the importance of this process for testing NP models in $B$ decays.

### 5.3 Combining observables

Above, we have seen that it is indeed possible to distinguish the $VB$ and $U_1$ models. $VB$ predicts that $\tau \to 3\mu$ is on the verge of being observed, while there are several other observables that are signals of $U_1$. Should one of these signals be seen, indicating the presence of a particular type of NP, it would of course be very exciting. However, even more information about the underlying NP model can be obtained by using the measurements of other observables.

The $U_1$ model contains three unknown parameters: $\theta_L$, $\theta_D$ and $|h^{33}_{U_1}|^2/\Lambda^2_{\rm NP}$. Then, given the measurement of an observable that indicates the presence of the $U_1$ model, one can use two other observables to derive the values of all the parameters of the model. To illustrate this, suppose that $R_K$ and $R_{D^{(*)}}$ are measured very precisely, and $R_K = 0.781$ and $R^{\rm ratio}_{D^{(*)}} = 1.077$ are found. If $\mathcal{B}(\Upsilon(3S) \to \mu\tau) = 1.11 \times 10^{-8}$ is also measured, this points to the $U_1$ model. The theoretical parameters must take the values $|h^{33}_{U_1}|^2/\Lambda^2_{\rm NP} = 2.43\,{\rm TeV}^{-2}$, $\theta_L = 0.039$, $\theta_D = 0.006$. $U_1$ then predicts $\mathcal{B}(B \to K^{(*)}\mu\tau) = 1.68 \times 10^{-8}$, $\mathcal{B}(B \to K^{(*)}\tau^+\tau^-) = 5.57 \times 10^{-6}$, $\mathcal{B}(B^0_s \to \mu\tau) = 2.80 \times 10^{-7}$, and $\mathcal{B}(B^0_s \to \tau^+\tau^-) = 2.57 \times 10^{-5}$.

On the other hand, the $VB$ model is much more restrictive. It contains four unknown parameters: $\theta_L$, $\theta_D$, $g^{33}_{qV}$ and $g^{33}_{lV}$ (without loss of generality we can set $\Lambda_{\rm NP} = 1\,{\rm TeV}$). Unlike the $U_1$ model, the $VB$ model receives severe constraints from $B^0_s$-$\bar{B}^0_s$ mixing and $\tau \to 3\mu$. The constraint from $B^0_s$-$\bar{B}^0_s$ mixing implies $g^{33}_{qV} \sin\theta_D \cos\theta_D < 4.2 \times 10^{-3}$, while the constraint from $\tau \to 3\mu$ implies $(g^{33}_{\ell V})^2 \sin^3\theta_L \cos\theta_L < 1.65 \times 10^{-2}$ at 90% C.L. These constraints leave no room for the $VB$ model to explain $R_K$ less than 0.90 at 90% or higher C.L.

## 6 Conclusions

At present, there are several measurements of $B$ decays that exhibit discrepancies with the predictions of the SM. These include $P'_5$ (from an angular analysis of $B \to K^*\mu^+\mu^-$), the differential branching fraction of $B^0_s \to \phi\mu^+\mu^-$, $R_K \equiv \mathcal{B}(B^+ \to K^+\mu^+\mu^-)/\mathcal{B}(B^+ \to K^+e^+e^-)$, and $R_{D^{(*)}} \equiv \mathcal{B}(\bar{B} \to D^{(*)}\tau^-\bar{\nu}_\tau)/\mathcal{B}(\bar{B} \to D^{(*)}\ell^-\bar{\nu}_\ell)$ $(\ell = e, \mu)$. These suggest NP

in $\bar{b} \to \bar{s}\mu^+\mu^-$ (first three signals) or $\bar{b} \to \bar{c}\tau^+\nu_\tau$ ($R_{D^{(*)}}$). Now, suppose that NP is present, and that it couples preferentially to the left-handed third-generation particles in the gauge basis. In ref. [30], it was noted that, if this NP is invariant under the full $\mathrm{SU}(3)_C \times \mathrm{SU}(2)_L \times \mathrm{U}(1)_Y$ gauge group, then, when one transforms to the mass basis, one generates the operators $(\bar{b}_L\gamma_\mu s_L)(\bar{\mu}_L\gamma^\mu\mu_L)$ (that contributes to $\bar{b} \to \bar{s}\mu^+\mu^-$) *and* $(\bar{b}_L\gamma_\mu c_L)(\bar{\tau}_L\gamma^\mu\nu_{\tau L})$ (that contributes to $\bar{b} \to \bar{c}\tau^+\nu_\tau$). In other words, the $R_K$ and $R_{D^{(*)}}$ puzzles can be simultaneously explained.

This idea was explored in greater detail, using an effective field theory approach, in ref. [44]. Here the starting point is a model-independent effective Lagrangian consisting of two four-fermion operators in the gauge basis, each with its own coupling. It was assumed that the transformation from the gauge basis to the mass basis leads to mixing only between the second and third generations. As a consequence, for the down-type quarks, only one unknown theoretical parameter is introduced: $\theta_D$. Similarly, for the charged leptons, $\theta_L$ is the new parameter. In the mass basis, the two operators contribute to a variety of $B$ decays, all with two quarks and two leptons at the fermion level: $B \to K^*\mu^+\mu^-$, $B_s^0 \to \phi\mu^+\mu^-$, $R_K$, $R_{D^{(*)}}$, $B \to K^{(*)}\nu\bar{\nu}$. The coefficients of the operators in the mass basis are all functions of the coupling$^2$, $\theta_D$ and $\theta_L$. For assumed values of the coupling$^2$, the experimental measurements lead to an allowed region in $(\theta_L, \theta_D)$ space. This region was found to be nonzero, showing that a simultaneous explanation of $R_K$ and $R_{D^{(*)}}$ is possible. There are two UV completions that can give rise to the effective Lagrangian. They are (i) $VB$: a vector boson that transforms as an $\mathrm{SU}(2)_L$ triplet, as in the SM, and (ii) $U_1$: an $\mathrm{SU}(2)_L$-singlet vector leptoquark.

The purpose of this paper is to explore ways of distinguishing the $VB$ and $U_1$ models. There are two reasons to think that this might be possible. First, the $VB$ model does not lead only to tree-level operators with two quarks and two leptons. It also produces four-quark and four-lepton operators. As such, it also contributes to processes such as $B_s^0$-$\bar{B}_s^0$ mixing and $\tau \to 3\mu$. These will lead to additional constraints on $\theta_D$ and $\theta_L$, respectively. Second, while $VB$ contributes to $B \to K^{(*)}\nu\bar{\nu}$, $U_1$ does not. The net effect is that the experimental constraints on the $VB$ model are more stringent than those on the $U_1$ model. That is, the allowed region in $(\theta_L, \theta_D)$ space is smaller for $VB$ than for $U_1$. This implies that the predictions for the rates of other lepton-flavor-violating processes may be very different in the two models, which will allow us to distinguish them.

With this in mind, our first step was to apply the relevant experimental constraints to determine the allowed region in $(\theta_L, \theta_D)$ space for each of the models. The constraints from the measurements of $R_K$, $R_D$, $R_{D^*}$, and $\tau \to \mu\phi$ applied to both models. For $VB$ there were additional constraints from $B \to K^{(*)}\nu\bar{\nu}$, $B_s^0$-$\bar{B}_s^0$ mixing, and $\tau \to 3\mu$.

Our intention was to then use the allowed $(\theta_L, \theta_D)$ regions to compute the predictions of the two models for various observables. However, the first step produced an unexpected result: the constraints on the $VB$ model are so stringent that it is just barely viable. To be specific, the boundaries of the allowed $(\theta_L, \theta_D)$ regions corresponding to the $\Delta M_s$, $b \to s\mu\mu$, and $\tau \to 3\mu$ constraints overlap at essentially a single point. This is a very different result than that found in the effective field theory analysis of ref. [44]. This is because all constraints have been included in the present model-dependent analysis. This



JHEP01(2017)015

illustrates that the results from the effective field theory analysis must be used carefully: despite being "model-independent," they do not necessarily apply to all models.

Things were very different for the $U_1$ model. We considered two possibilities for the coupling[2]: $\left|h_{U_1}^{33}\right|^2 = 1$ and $0.5 \leq \left|h_{U_1}^{33}\right|^2 \leq 5$. In either case, the allowed region in $(\theta_L, \theta_D)$ space is sizeable.

For both models, using the allowed $(\theta_L, \theta_D)$ regions, we then computed the predictions for various observables. Note that, since the $(\theta_L, \theta_D)$ "region" of the $VB$ model consists essentially of a single point, the predictions for the observables are very specific. On the other hand, the $U_1$ model gives ranges for its predictions. The observables include $R_{D^{(*)}}$, $R_K$, $\tau \to 3\mu$ ($VB$ only), $B \to K^{(*)}\mu\tau$, $B \to K^{(*)}\tau^+\tau^-$, $B_s^0 \to \mu\tau$, $B_s^0 \to \tau^+\tau^-$ and $\Upsilon(3S) \to \mu\tau$. Note that the lepton-flavor-violating decay $\Upsilon(3S) \to \mu\tau$ has been overlooked in previous analyses. However, it is potentially an important process for testing models proposed to explain the $B$-decay anomalies.

Given that their allowed $(\theta_L, \theta_D)$ regions are so different, it is indeed possible to distinguish the $VB$ and $U_1$ models experimentally. $VB$ predicts $\mathcal{B}(\tau^- \to \mu^-\mu^+\mu^-) \simeq 2.1 \times 10^{-8}$, which is the present upper limit. This is measurable at Belle II and LHCb, so that $\tau \to 3\mu$ constitutes a smoking-gun signal for the $VB$ model. There is no similar observable for the $U_1$ model. However, there are a number of processes that can potentially point to $U_1$. We present the results for $0.5 \leq \left|h_{U_1}^{33}\right|^2 \leq 5$. For the decay $\Upsilon(3S) \to \mu\tau$, we estimated that Belle II should be able to measure its branching ratio down to $\sim 10^{-7}$. But the $U_1$ ($VB$) model predicts $\mathcal{B}(\Upsilon(3S) \to \mu\tau)|_{\max} = 8.0 \times 10^{-7}$ ($3.0 \times 10^{-9}$). Thus, if this decay were observed, it would indicate $U_1$ (and exclude $VB$). Another possibility is $R_K$. Its present allowed $3\sigma$ range is $0.498 \leq R_K \leq 1.036$. The $U_1$ ($VB$) model predicts $0.51 \leq R_K \leq 0.90$ ($R_K \simeq 0.90$). The $U_1$ model can therefore accomodate smaller values of $R_K$ than can the $VB$ model, so that, if future measurements find $0.51 \leq R_K < 0.90$ at higher than 90% C.L., this would exclude $VB$ and favor $U_1$. Finally, for the other decays $B \to K^{(*)}\mu\tau$, $B \to K^{(*)}\tau^+\tau^-$, $B_s^0 \to \mu\tau$, and $B_s^0 \to \tau^+\tau^-$, in all cases the $U_1$ model predicts larger branching ratios than does $VB$. However, whether or not these decays can be used to distinguish the two models depends on whether they can be observed at Belle II or LHCb.

**Notes added.** (1) While this paper was being completed, the Belle Collaboration released a new measurement of $R_{D^*}$ [84]. They find consistency with the SM at the level of $0.6\sigma$. Now, if this result is combined with the previous results of BaBar, Belle and LHCb, the discrepancy with the SM is reduced. However, in any case, neither of the $VB$ and $U_1$ models presented in this paper allows for large deviations in $R_{D^{(*)}}$ from the SM. Thus, this result is rather favored. (2) After this paper was submitted to the arXiv, we were informed that LHCb has now set the upper limit $\mathcal{B}(B_s^0 \to \tau^+\tau^-) < 3.0 \times 10^{-3}$ (95% C.L.) [85].

## Acknowledgments

We thank S. Robertson and P. Urquijo for information about the reach of Belle II, and E. Ben-Haim, T. Gershon, F. Polci and J. Serrano for information about the reach of LHCb. We thank some people for bringing to our attention certain references: G. Isidori



JHEP01(2017)015

(refs. [18, 56]), J. Serrano (ref. [85]). DL thanks R. Chouiab and S. Robertson for helpful discussions about the experimental measurement of $B \to K\tau^+\tau^-$. RW thanks A. Ishikawa for discussions about the experimental measurement of $B_s \to \tau^+\tau^-$ at Belle II. RW is grateful to Kenji Nishiwaki for giving us a critical question so that we could discover an error in our fitting program. This work was financially supported by NSERC of Canada (BB, JPG, DL), and by the National Science Foundation (AD) under Grant No. NSF PHY-1414345. BB acknowledges partial support from the U. S. Department of Energy under contract DE-SC0007983. This work was supported by IBS under the project code, IBS-R018-D1 (RW). AD acknowledges the hospitality of the Department of Physics and Astronomy, University of Hawaii, where part of the work was done.



JHEP01(2017)015

## References

[1] LHCb collaboration, *Measurement of Form-Factor-Independent Observables in the Decay* $B^0 \to K^{*0}\mu^+\mu^-$, *Phys. Rev. Lett.* **111** (2013) 191801 [arXiv:1308.1707] [INSPIRE].

[2] LHCb collaboration, *Angular analysis of the* $B^0 \to K^{*0}\mu^+\mu^-$ *decay using 3* $fb^{-1}$ *of integrated luminosity*, *JHEP* **02** (2016) 104 [arXiv:1512.04442] [INSPIRE].

[3] U. Egede, T. Hurth, J. Matias, M. Ramon and W. Reece, *New observables in the decay mode* $\bar{B}_d \to \bar{K}^{*0}l^+l^-$, *JHEP* **11** (2008) 032 [arXiv:0807.2589] [INSPIRE].

[4] BELLE collaboration, A. Abdesselam et al., *Angular analysis of* $B^0 \to K^*(892)^0\ell^+\ell^-$, arXiv:1604.04042 [INSPIRE].

[5] S. Descotes-Genon, T. Hurth, J. Matias and J. Virto, *Optimizing the basis of* $B \to K^*ll$ *observables in the full kinematic range*, *JHEP* **05** (2013) 137 [arXiv:1303.5794] [INSPIRE].

[6] S. Descotes-Genon, L. Hofer, J. Matias and J. Virto, *On the impact of power corrections in the prediction of* $B \to K^*\mu^+\mu^-$ *observables*, *JHEP* **12** (2014) 125 [arXiv:1407.8526] [INSPIRE].

[7] J. Lyon and R. Zwicky, *Resonances gone topsy turvy — the charm of QCD or new physics in* $b \to s\ell^+\ell^-$ *?*, arXiv:1406.0566 [INSPIRE].

[8] S. Jäger and J. Martin Camalich, *Reassessing the discovery potential of the* $B \to K^*\ell^+\ell^-$ *decays in the large-recoil region: SM challenges and BSM opportunities*, *Phys. Rev.* **D 93** (2016) 014028 [arXiv:1412.3183] [INSPIRE].

[9] M. Ciuchini, M. Fedele, E. Franco, S. Mishima, A. Paul, L. Silvestrini et al., $B \to K^*\ell^+\ell^-$ *decays at large recoil in the Standard Model: a theoretical reappraisal*, *JHEP* **06** (2016) 116 [arXiv:1512.07157] [INSPIRE].

[10] S. Descotes-Genon, L. Hofer, J. Matias and J. Virto, *Global analysis of* $b \to s\ell\ell$ *anomalies*, *JHEP* **06** (2016) 092 [arXiv:1510.04239] [INSPIRE].

[11] T. Hurth, F. Mahmoudi and S. Neshatpour, *On the anomalies in the latest LHCb data*, *Nucl. Phys.* **B 909** (2016) 737 [arXiv:1603.00865] [INSPIRE].

[12] LHCb collaboration, *Differential branching fraction and angular analysis of the decay* $B_s^0 \to \phi\mu^+\mu^-$, *JHEP* **07** (2013) 084 [arXiv:1305.2168] [INSPIRE].

[13] LHCb collaboration, *Angular analysis and differential branching fraction of the decay* $B_s^0 \to \phi\mu^+\mu^-$, *JHEP* **09** (2015) 179 [arXiv:1506.08777] [INSPIRE].

[14] R.R. Horgan, Z. Liu, S. Meinel and M. Wingate, *Calculation of* $B^0 \to K^{*0}\mu^+\mu^-$ *and* $B_s^0 \to \phi\mu^+\mu^-$ *observables using form factors from lattice QCD*, *Phys. Rev. Lett.* **112** (2014) 212003 [arXiv:1310.3887] [INSPIRE].

[15] R.R. Horgan, Z. Liu, S. Meinel and M. Wingate, *Rare B decays using lattice QCD form factors*, PoS(LATTICE2014)372 [arXiv:1501.00367] [INSPIRE].

[16] A. Bharucha, D.M. Straub and R. Zwicky, $B \to V\ell^+\ell^-$ *in the Standard Model from light-cone sum rules*, *JHEP* **08** (2016) 098 [arXiv:1503.05534] [INSPIRE].

[17] LHCb collaboration, *Test of lepton universality using* $B^+ \to K^+\ell^+\ell^-$ *decays*, *Phys. Rev. Lett.* **113** (2014) 151601 [arXiv:1406.6482] [INSPIRE].

[18] M. Bordone, G. Isidori and A. Pattori, *On the Standard Model predictions for* $R_K$ *and* $R_{K^*}$, *Eur. Phys. J.* **C 76** (2016) 440 [arXiv:1605.07633] [INSPIRE].

[19] BABAR collaboration, J.P. Lees et al., *Measurement of an Excess of* $\bar{B} \to D^{(*)}\tau^-\bar{\nu}_\tau$ *Decays and Implications for Charged Higgs Bosons*, *Phys. Rev.* **D 88** (2013) 072012 [arXiv:1303.0571] [INSPIRE].

[20] BELLE collaboration, M. Huschle et al., *Measurement of the branching ratio of* $\bar{B} \to D^{(*)}\tau^-\bar{\nu}_\tau$ *relative to* $\bar{B} \to D^{(*)}\ell^-\bar{\nu}_\ell$ *decays with hadronic tagging at Belle*, *Phys. Rev.* **D 92** (2015) 072014 [arXiv:1507.03233] [INSPIRE].

[21] LHCb collaboration, *Measurement of the ratio of branching fractions* $\mathcal{B}(\bar{B}^0 \to D^{*+}\tau^-\bar{\nu}_\tau)/\mathcal{B}(\bar{B}^0 \to D^{*+}\mu^-\bar{\nu}_\mu)$, *Phys. Rev. Lett.* **115** (2015) 111803 [*Addendum ibid.* **115** (2015) 159901] [arXiv:1506.08614] [INSPIRE].

[22] B. Dumont, K. Nishiwaki and R. Watanabe, *LHC constraints and prospects for* $S_1$ *scalar leptoquark explaining the* $\bar{B} \to D^{(*)}\tau\bar{\nu}$ *anomaly*, *Phys. Rev.* **D 94** (2016) 034001 [arXiv:1603.05248] [INSPIRE].

[23] M. Tanaka and R. Watanabe, *New physics in the weak interaction of* $\bar{B} \to D^{(*)}\tau\bar{\nu}$, *Phys. Rev.* **D 87** (2013) 034028 [arXiv:1212.1878] [INSPIRE].

[24] A. Datta, M. Duraisamy and D. Ghosh, *Explaining the* $B \to K^*\mu^+\mu^-$ *data with scalar interactions*, *Phys. Rev.* **D 89** (2014) 071501 [arXiv:1310.1937] [INSPIRE].

[25] G. Hiller and M. Schmaltz, $R_K$ *and future* $b \to s\ell\ell$ *physics beyond the standard model opportunities*, *Phys. Rev.* **D 90** (2014) 054014 [arXiv:1408.1627] [INSPIRE].

[26] D. Ghosh, M. Nardecchia and S.A. Renner, *Hint of Lepton Flavour Non-Universality in B Meson Decays*, *JHEP* **12** (2014) 131 [arXiv:1408.4097] [INSPIRE].

[27] T. Hurth, F. Mahmoudi and S. Neshatpour, *Global fits to* $b \to s\ell\ell$ *data and signs for lepton non-universality*, *JHEP* **12** (2014) 053 [arXiv:1410.4545] [INSPIRE].

[28] W. Altmannshofer and D.M. Straub, *New physics in* $b \to s$ *transitions after LHC run 1*, *Eur. Phys. J.* **C 75** (2015) 382 [arXiv:1411.3161] [INSPIRE].

[29] S.L. Glashow, D. Guadagnoli and K. Lane, *Lepton Flavor Violation in B Decays?*, *Phys. Rev. Lett.* **114** (2015) 091801 [arXiv:1411.0565] [INSPIRE].

JHEP01(2017)015

[30] B. Bhattacharya, A. Datta, D. London and S. Shivashankara, *Simultaneous Explanation of the $R_K$ and $R_{D^{(*)}}$ Puzzles*, *Phys. Lett.* **B 742** (2015) 370 [arXiv:1412.7164] [INSPIRE].

[31] A. Datta, M. Duraisamy and D. Ghosh, *Diagnosing New Physics in $b \to c\tau\nu_\tau$ decays in the light of the recent BaBar result*, *Phys. Rev.* **D 86** (2012) 034027 [arXiv:1206.3760] [INSPIRE].

[32] A. Celis, M. Jung, X.-Q. Li and A. Pich, *Sensitivity to charged scalars in $B \to D^{(*)}\tau\nu_\tau$ and $B \to \tau\nu_\tau$ decays*, *JHEP* **01** (2013) 054 [arXiv:1210.8443] [INSPIRE].

[33] A. Crivellin, A. Kokulu and C. Greub, *Flavor-phenomenology of two-Higgs-doublet models with generic Yukawa structure*, *Phys. Rev.* **D 87** (2013) 094031 [arXiv:1303.5877] [INSPIRE].

[34] I. Doršner, S. Fajfer, N. Košnik and I. Nišandžić, *Minimally flavored colored scalar in $\bar{B} \to D^{(*)}\tau\bar{\nu}$ and the mass matrices constraints*, *JHEP* **11** (2013) 084 [arXiv:1306.6493] [INSPIRE].

[35] M. Freytsis, Z. Ligeti and J.T. Ruderman, *Flavor models for $\bar{B} \to D^{(*)}\tau\bar{\nu}$*, *Phys. Rev.* **D 92** (2015) 054018 [arXiv:1506.08896] [INSPIRE].

[36] N.G. Deshpande and X.-G. He, *Consequences of R-Parity violating interactions for anomalies in $\bar{B} \to D^{(*)}\tau\bar{\nu}$ and $b \to s\mu^+\mu^-$*, arXiv:1608.04817 [INSPIRE].

[37] M.A. Ivanov, J.G. Körner and C.-T. Tran, *Analyzing new physics in the decays $\bar{B}^0 \to D^{(*)}\tau^-\bar{\nu}_\tau$ with form factors obtained from the covariant quark model*, *Phys. Rev.* **D 94** (2016) 094028 [arXiv:1607.02932] [INSPIRE].

[38] M. Duraisamy and A. Datta, *The Full $B \to D^*\tau^-\bar{\nu_\tau}$ Angular Distribution and CP-violating Triple Products*, *JHEP* **09** (2013) 059 [arXiv:1302.7031] [INSPIRE].

[39] M. Duraisamy, P. Sharma and A. Datta, *Azimuthal $B \to D^*\tau^-\bar{\nu_\tau}$ angular distribution with tensor operators*, *Phys. Rev.* **D 90** (2014) 074013 [arXiv:1405.3719] [INSPIRE].

[40] Y. Sakaki, M. Tanaka, A. Tayduganov and R. Watanabe, *Probing New Physics with $q^2$ distributions in $\bar{B} \to D^{(*)}\tau\bar{\nu}$*, *Phys. Rev.* **D 91** (2015) 114028 [arXiv:1412.3761] [INSPIRE].

[41] D. Das, C. Hati, G. Kumar and N. Mahajan, *Towards a unified explanation of $R_{D^{(*)}}$, $R_K$ and $(g-2)_\mu$ anomalies in a left-right model with leptoquarks*, *Phys. Rev.* **D 94** (2016) 055034 [arXiv:1605.06313] [INSPIRE].

[42] C.-J. Lee and J. Tandean, *Minimal lepton flavor violation implications of the $b \to s$ anomalies*, *JHEP* **08** (2015) 123 [arXiv:1505.04692] [INSPIRE].

[43] D. Bečirević, S. Fajfer and N. Košnik, *Lepton flavor nonuniversality in $b \to sl^+l^-$ processes*, *Phys. Rev.* **D 92** (2015) 014016 [arXiv:1503.09024] [INSPIRE].

[44] L. Calibbi, A. Crivellin and T. Ota, *Effective field theory approach to $b \to s\ell\ell^{(\prime)}$, $B \to K^{(*)}\nu\bar{\nu}$ and $B \to D^{(*)}\tau\nu$ with third generation couplings*, *Phys. Rev. Lett.* **115** (2015) 181801 [arXiv:1506.02661] [INSPIRE].

[45] BABAR collaboration, J.P. Lees et al., *Search for $B \to K^{(*)}\nu\bar{\nu}$ and invisible quarkonium decays*, *Phys. Rev.* **D 87** (2013) 112005 [arXiv:1303.7465] [INSPIRE].

[46] BELLE collaboration, O. Lutz et al., *Search for $B \to h^{(*)}\nu\bar{\nu}$ with the full Belle $\Upsilon(4S)$ data sample*, *Phys. Rev.* **D 87** (2013) 111103 [arXiv:1303.3719] [INSPIRE].

[47] R. Alonso, B. Grinstein and J. Martin Camalich, *Lepton universality violation and lepton flavor conservation in B-meson decays*, *JHEP* **10** (2015) 184 [arXiv:1505.05164] [INSPIRE].




JHEP01(2017)015

[48] A. Crivellin, G. D'Ambrosio and J. Heeck, *Addressing the LHC flavor anomalies with horizontal gauge symmetries*, *Phys. Rev.* **D 91** (2015) 075006 [arXiv:1503.03477] [INSPIRE].

[49] A. Greljo, G. Isidori and D. Marzocca, *On the breaking of Lepton Flavor Universality in B decays*, *JHEP* **07** (2015) 142 [arXiv:1506.01705] [INSPIRE].

[50] D. Aristizabal Sierra, F. Staub and A. Vicente, *Shedding light on the $b \to s$ anomalies with a dark sector*, *Phys. Rev.* **D 92** (2015) 015001 [arXiv:1503.06077] [INSPIRE].

[51] C.-W. Chiang, X.-G. He and G. Valencia, *$Z'$ model for $b \to s\ell\bar{\ell}$ flavor anomalies*, *Phys. Rev.* **D 93** (2016) 074003 [arXiv:1601.07328] [INSPIRE].

[52] S.M. Boucenna, A. Celis, J. Fuentes-Martin, A. Vicente and J. Virto, *Non-abelian gauge extensions for B-decay anomalies*, *Phys. Lett.* **B 760** (2016) 214 [arXiv:1604.03088] [INSPIRE].

[53] Y. Sakaki, M. Tanaka, A. Tayduganov and R. Watanabe, *Testing leptoquark models in $\bar{B} \to D^{(*)}\tau\bar{\nu}$*, *Phys. Rev.* **D 88** (2013) 094012 [arXiv:1309.0301] [INSPIRE].

[54] B. Gripaios, M. Nardecchia and S.A. Renner, *Composite leptoquarks and anomalies in B-meson decays*, *JHEP* **05** (2015) 006 [arXiv:1412.1791] [INSPIRE].

[55] I. de Medeiros Varzielas and G. Hiller, *Clues for flavor from rare lepton and quark decays*, *JHEP* **06** (2015) 072 [arXiv:1503.01084] [INSPIRE].

[56] R. Barbieri, G. Isidori, A. Pattori and F. Senia, *Anomalies in B-decays and $U(2)$ flavour symmetry*, *Eur. Phys. J.* **C 76** (2016) 67 [arXiv:1512.01560] [INSPIRE].

[57] S. Fajfer and N. Košnik, *Vector leptoquark resolution of $R_K$ and $R_{D^{(*)}}$ puzzles*, *Phys. Lett.* **B 755** (2016) 270 [arXiv:1511.06024] [INSPIRE].

[58] S. Sahoo, R. Mohanta and A.K. Giri, *Explaining $R_K$ and $R_{D^{(*)}}$ anomalies with vector leptoquark*, arXiv:1609.04367 [INSPIRE].

[59] A.J. Buras, J. Girrbach-Noe, C. Niehoff and D.M. Straub, *$B \to K^{(*)}\nu\overline{\nu}$ decays in the Standard Model and beyond*, *JHEP* **02** (2015) 184 [arXiv:1409.4557] [INSPIRE].

[60] ALEPH collaboration, R. Barate et al., *Measurements of $BR(b \to \tau^-\bar{\nu}_\tau X)$ and $BR(b \to \tau^-\bar{\nu}_\tau D^{*\pm} X)$ and upper limits on $BR(B^- \to \tau^-\bar{\nu}_\tau)$ and $BR(b \to s\bar{\nu})$*, *Eur. Phys. J.* **C 19** (2001) 213 [hep-ex/0010022] [INSPIRE].

[61] PARTICLE DATA GROUP collaboration, K.A. Olive et al., *Review of Particle Physics*, *Chin. Phys.* **C 38** (2014) 090001 [INSPIRE].

[62] A. Datta, X.G. He and S. Pakvasa, *Quasiinclusive and exclusive decays of B to eta-prime*, *Phys. Lett.* **B 419** (1998) 369 [hep-ph/9707259] [INSPIRE].

[63] B. Bhattacharya and J.L. Rosner, *Effect of $\eta$-$\eta'$ mixing on $D \to PV$ decays*, *Phys. Rev.* **D 82** (2010) 037502 [arXiv:1005.2159] [INSPIRE].

[64] BELLE collaboration, Y. Miyazaki et al., *Search for Lepton-Flavor-Violating tau Decays into a Lepton and a Vector Meson*, *Phys. Lett.* **B 699** (2011) 251 [arXiv:1101.0755] [INSPIRE].

[65] G. Buchalla, A.J. Buras and M.E. Lautenbacher, *Weak decays beyond leading logarithms*, *Rev. Mod. Phys.* **68** (1996) 1125 [hep-ph/9512380] [INSPIRE].

[66] S. Aoki et al., *Review of lattice results concerning low-energy particle physics*, *Eur. Phys. J.* **C 74** (2014) 2890 [arXiv:1310.8555] [INSPIRE].

JHEP01(2017)015

[67] S. Aoki et al., *Review of lattice results concerning low-energy particle physics*, arXiv:1607.00299 [INSPIRE].

[68] J. Charles et al., *Current status of the Standard Model CKM fit and constraints on $\Delta F = 2$ New Physics*, *Phys. Rev.* **D 91** (2015) 073007 [arXiv:1501.05013] [INSPIRE].

[69] K.G. Chetyrkin, J.H. Kuhn and M. Steinhauser, *RunDec: A Mathematica package for running and decoupling of the strong coupling and quark masses*, *Comput. Phys. Commun.* **133** (2000) 43 [hep-ph/0004189] [INSPIRE].

[70] HEAVY FLAVOR AVERAGING GROUP (HFAG) collaboration, Y. Amhis et al., *Averages of b-hadron, c-hadron and $\tau$-lepton properties as of summer 2014*, arXiv:1412.7515 [INSPIRE].

[71] K. Hayasaka et al., *Search for Lepton Flavor Violating Tau Decays into Three Leptons with 719 Million Produced Tau+Tau- Pairs*, *Phys. Lett.* **B 687** (2010) 139 [arXiv:1001.3221] [INSPIRE].

[72] F. Feruglio, P. Paradisi and A. Pattori, *Revisiting Lepton Flavour Universality in B Decays*, arXiv:1606.00524 [INSPIRE].

[73] David Straub, *flavio v0.11, 2016*, http://dx.doi.org/10.5281/zenodo.59840.

[74] J.-G. Shiu (National Taiwan University) on behalf of the Belle II collaboration, *BelleII: physics and early measurements*, talk given at *Beauty 2016*, Marseille, France, https://indico.cern.ch/event/352928/contributions/1757317.

[75] LHCb collaboration, *Letter of Intent for the LHCb Upgrade*, CERN-LHCC-2011-001.

[76] BABAR collaboration, B. Aubert et al., *Search for the decay $B^+ \to K^+\tau^\mp\mu^\pm$*, *Phys. Rev. Lett.* **99** (2007) 201801 [arXiv:0708.1303] [INSPIRE].

[77] S. Robertson and P. Urquijo, private communication.

[78] BABAR collaboration, J.P. Lees et al., *Search for $B^+ \to K^+\tau^+\tau^-$ at the BaBar experiment*, arXiv:1605.09637 [INSPIRE].

[79] T. Gershon, F. Polci and J. Serrano, private communication.

[80] A. Datta, P.J. O'Donnell, S. Pakvasa and X. Zhang, *Flavor changing processes in quarkonium decays*, *Phys. Rev.* **D 60** (1999) 014011 [hep-ph/9812325] [INSPIRE].

[81] BABAR collaboration, J.P. Lees et al., *Search for Charged Lepton Flavor Violation in Narrow Upsilon Decays*, *Phys. Rev. Lett.* **104** (2010) 151802 [arXiv:1001.1883] [INSPIRE].

[82] CLEO collaboration, W. Love et al., *Search for Lepton Flavor Violation in Upsilon Decays*, *Phys. Rev. Lett.* **101** (2008) 201601 [arXiv:0807.2695] [INSPIRE].

[83] D.A. Faroughy, A. Greljo and J.F. Kamenik, *Confronting lepton flavor universality violation in B decays with high-$p_T$ tau lepton searches at LHC*, *Phys. Lett.* **B 764** (2017) 126 [arXiv:1609.07138] [INSPIRE].

[84] A. Abdesselam et al., *Measurement of the $\tau$ lepton polarization in the decay $\bar{B} \to D^*\tau^-\bar{\nu}_\tau$*, arXiv:1608.06391 [INSPIRE].

[85] K. De Bruyn (LHCb Collaboration), *Tests of Lepton Universality at LHCb*, talk at TAU2016, LHCb-CONF-2016-011, http://indico.ihep.ac.cn/event/5221/session/12/contribution/69/material/slides/0.pdf.



JHEP01(2017)015